

Detecting the polarization in $\chi_{cJ} \rightarrow \phi\phi$ decays to probe hadronic loop effect

Qi Huang,^{1,*} Jun-Zhang Wang,^{2,3,†} Rong-Gang Ping,^{1,4,‡} and Xiang Liu^{2,3,5,§}

¹University of Chinese Academy of Sciences (UCAS), Beijing 100049, China

²School of Physical Science and Technology, Lanzhou University, Lanzhou 730000, China

³Research Center for Hadron and CSR Physics,

Lanzhou University and Institute of Modern Physics of CAS, Lanzhou 730000, China

⁴Institute of High Energy Physics, Chinese Academy of Sciences, P.O. Box 918(1), Beijing 100049, China

⁵Lanzhou Center for Theoretical Physics, Key Laboratory of Theoretical Physics of Gansu Province, and Frontiers Science Center for Rare Isotopes, Lanzhou University, Lanzhou 730000, China



(Received 16 February 2021; accepted 13 April 2021; published 10 May 2021)

In this work, we show that detecting the polarization information of $\chi_{cJ} \rightarrow \phi\phi (J = 0, 1, 2)$ could be a practical way to test the hadronic loop effect in these decays. Our results show that the predicted ratios of helicity amplitudes are less dependent on the parameters involved in the calculation. The ratios are determined to be $|F_{1,1}^{(0)}/F_{0,0}^{(0)}| \approx 0.359$, $|F_{1,0}^{(1)}/F_{0,1}^{(1)}| = 1$, $|F_{1,1}^{(1)}/F_{0,1}^{(1)}| = 0$, $|F_{1,0}^{(2)}/F_{0,0}^{(2)}| = |F_{0,1}^{(2)}/F_{0,0}^{(2)}| \approx 1.285$, $|F_{1,-1}^{(2)}/F_{0,0}^{(2)}| = |F_{-1,1}^{(2)}/F_{0,0}^{(2)}| \approx 5.110$, and $|F_{-1,-1}^{(2)}/F_{0,0}^{(2)}| = |F_{1,1}^{(2)}/F_{0,0}^{(2)}| \approx 0.465$. By adopting these predicted ratios, we use the Monte Carlo events to show that the moments $\langle t_{ij} \rangle$ can be used as observables to reveal the polarization transfer in these decays, and their distributions are directly related to the determination of helicity amplitudes. We suggest experiments like at the BESIII and the Belle II performing a polarization analysis on the $\chi_{cJ} \rightarrow \phi\phi$ decay in the future, and the results are important to understand the decay mechanism underlying the χ_{cJ} decays.

DOI: 10.1103/PhysRevD.103.096006

I. INTRODUCTION

How to quantitatively depict nonperturbative behavior of strong interaction at the medium and low energy region is a great challenge for us to understand the hadronic confinement and the related hadron properties. Though the foundation of lattice QCD has well established and commonly accepted as a reliable way to deal with these issues, its development is relatively slow compared to the accumulations of experimental data in last two decades [1–5]. In recent years, more and more exotic hadronic states and exotic decays are reported, which enriches our knowledge about the hadron spectroscopy [6–10]. To reveal the mechanisms underlying these new structures and their decay properties, the effective theory, QCD sum rule and other phenomenological methods are indispensable for bridging the strong interactions to the hadron nonperturbative properties.

Since the discovery of J/ψ particle in 1974, the charm physics has been continuing to be the laboratory to study the properties of light hadron, charmed meson, and charmonium. In this work, we suggest the experiments to measure the polarization transfer in the $\psi(2S) \rightarrow \gamma\chi_{cJ}$, $\chi_{cJ} \rightarrow \phi\phi$ to figure out the decay mechanism of χ_{cJ} . Experimentally, the ϕ mesons can be reconstructed with the Kaon charged tracks registered in the detector. The narrow width of the χ_{cJ} and ϕ mesons provide a beneficial selection criteria to reconstruct the decay chain. The branching fractions for the charmonium transition $\psi(2S) \rightarrow \gamma\chi_{cJ} (J = 0, 1, 2)$ are summed up to about 30%, hence this transition could be the χ_{cJ} factory, which can produce a large size of χ_{cJ} events. For example, with accumulation of 3 billion $\psi(2S)$ events in the future [11], it will produce 0.9 billion χ_{cJ} events. The large size of χ_{cJ} sample is essential to analyze the polarization transfer, since the experiment is dependent on the observation of polarization moments, which are constructed with the helicity angles in the cascade decays.

The $\chi_{c1} \rightarrow \phi\phi$ decay was first reported by the BESIII Collaboration in 2011 [12]. With observed 254 events in the $\phi\phi$ mass spectrum, its branching fraction was significantly measured with the same order as that for the $\chi_{c0} \rightarrow \phi\phi$ decay [12,13]. This puts a great challenge for the theoretical investigation on its decay mechanism in the pQCD scenario. Since the strong decay conserves the

*huangqi@ucas.ac.cn

†wangjzh2012@lzu.edu.cn

‡pingrg@ihep.ac.cn

§xiangliu@lzu.edu.cn

Published by the American Physical Society under the terms of the Creative Commons Attribution 4.0 International license. Further distribution of this work must maintain attribution to the author(s) and the published article's title, journal citation, and DOI. Funded by SCOAP³.

parity, there is a strong constraint on the helicity selection rule for the $\chi_{c1} \rightarrow \phi(\lambda_1)\phi(\lambda_2)$ decay, here λ_1, λ_2 denote the helicity values of ϕ mesons. Besides, there exists a further constraint, which is due to the requirement on the identical particle symmetry of $\phi\phi$ system. These constraints result in the helicity amplitude vanishing with helicity selection rule $\lambda_1 = \lambda_2$. The nonvanishing helicity amplitudes are those with $(\lambda_1, \lambda_2) = (\pm 1, 0)$ or $(0, \pm 1)$. However, these helicity configurations violate the helicity selection rule in the χ_{c1} decay. Their contributions to the partial decay width is suppressed by a factor of $(\Lambda_{\text{QCD}}/m_c)^6$, here m_c is the mass of charm quark, and Λ_{QCD} is the QCD energy scale. This strong suppression can be simply understood according to the Landau-Yang theorem [14].

The same situation happens in the $\chi_{c2} \rightarrow \phi(\lambda_1)\phi(\lambda_2)$ decay [15]. The parity conservation and identical particle symmetry allow the existence of the nonvanishing amplitude for all helicity configurations with $|\lambda_1 - \lambda_2| \leq 2$, but the helicity selection rule results in a suppression factor to the branching fraction according to the pQCD asymptotic behavior [16], i.e.,

$$\mathcal{B}(\chi_{c2} \rightarrow \phi(\lambda_1)\phi(\lambda_2)) \sim \left(\frac{\Lambda_{\text{QCD}}^2}{m_c^2}\right)^{|\lambda_1 + \lambda_2| + 2}. \quad (1)$$

The pQCD calculation determined its branching fraction to be $\mathcal{B}(\chi_{c2} \rightarrow \phi\phi) = 7.8 \times 10^{-4}$ [17], which is less than the average of measured ones, $(1.06 \pm 0.09) \times 10^{-3}$ [13], by about 30%.

To decode the nonperturbative mechanism underlying these decays, the hadronic loop mechanism (HLM) [18–39] was introduced in Refs. [21,22]. In this scenario, the $\phi\phi$ production is supposed to be from the rescattering of two virtual charmed mesons by exchanging another charmed meson. It shows that under HLM the measured branching ratios can be well reproduced within experimental uncertainty. To some extent one can expect that the hadronic loop mechanism can model the long distance effects in the χ_{cJ} decays. However, to comprehensively test the hadronic loop mechanism, it is desirable to give more predictions on the χ_{cJ} decays besides the branching fraction.

In this work, we show that detecting the polarization information of $\chi_{cJ} \rightarrow \phi\phi$ can be an effective way to probe hadronic loop mechanism. Especially in the χ_{c2} decays, the two ϕ decays provide us with rich spin observables. In the HLM scenario, these spin observables can be predicted by calculating the helicity amplitudes. The suppression of helicity selection rule is characterized by the ratios between the amplitudes of the ϕ longitudinal polarization components. Thus, experimental measurements on the ratios of helicity amplitudes can provide us with a very good platform to test if there exists the long distance contributions to the $\chi_{cJ} \rightarrow \phi\phi$ decays. With this motivation, we present a polarization analysis on the $\chi_{cJ} \rightarrow \phi\phi$ decays in the HLM scenario. We find that the obtained ratios of

helicity amplitudes is less dependent on the parameters, i.e., their values change little with variations of the free parameters in the model. An ensemble of Monte Carlo (MC) events are generated based on the amplitude ratios, and we show that some moments $\langle t_{ij} \rangle$ can be used as polarization observables. With this investigation, we strongly suggest the BESIII and Belle II to perform a measurement on the polarization in the $\chi_{cJ} \rightarrow \phi\phi$ decays, which may provide crucial tests to the hadronic loop mechanism.

This paper is organized as follows. After the introduction, we present a polarization analysis of the decay $\chi_{cJ} \rightarrow \phi\phi \rightarrow 2(K^+K^-)$ in Sec. II. Then, the calculation of $\chi_{cJ} \rightarrow \phi\phi$ in the charmed meson loop scenario is presented in Sec. III. The numerical results are given in Sec. IV. Finally, this paper ends with a summary.

II. POLARIZATION ANALYSIS

We analyze the $\phi\phi$ polarization started with e^+e^- beams. In the unpolarized e^+e^- collider, the production of $\psi(2S)$ particle is tensor polarized without longitudinal polarization [40]. Thus, the subsequent $\psi(2S) \rightarrow \gamma\chi_{cJ}$ decay may transfer some polarization to the χ_{cJ} states, which is manifested in the $\chi_{cJ} \rightarrow \phi\phi$ decay, showing up with an unflat angular distribution of the decayed ϕ meson.

To get the polarization or alignment information of $\phi\phi$ system, one has to investigate its spin density matrix (SDM), which encodes the full polarization information transferred from the χ_{cJ} decays. In experiment, the measurement on the $\phi\phi$ SDM plays the role to study the χ_{cJ} decay mechanism, given that the polarization pattern is predicted based on the decay-dynamical models. We follow the standard way to construct the SDM for the identical particle $\phi\phi$ system.

For a spin- s particle, its spin density matrix is given in terms of multipole parameters, r_M^L , as [41]

$$\rho = \frac{1}{2s+1} \left(\mathcal{I} + 2s \sum_{L=1}^{2s} \sum_{M=-L}^L r_M^L Q[s, L, M] \right), \quad (2)$$

where \mathcal{I} denotes a $(2s+1) \times (2s+1)$ dimensional unit matrix, L is the orbital angular momentum with its magnetic quantum number M defined in the spherical tensor operator. The SDM for $\phi\phi$ system can be constructed from the ϕ individual ones, and an easy way is to decompose it into Q matrices multiplied by a set of real parameters, which reads as

$$\begin{aligned} \rho_{\phi\phi} &= \rho_\phi \otimes \rho_\phi \\ &= \frac{1}{9} \left[C_{00} \mathcal{I}_3 \otimes \mathcal{I}_3 + 2 \sum_{i=1}^8 (C_{i,0} Q_i \otimes \mathcal{I}_3 \right. \\ &\quad \left. + C_{0i} \mathcal{I}_3 \otimes Q_i) + 4 \sum_{i,j=1}^8 C_{ij} Q_i \otimes Q_j \right]. \quad (3) \end{aligned}$$

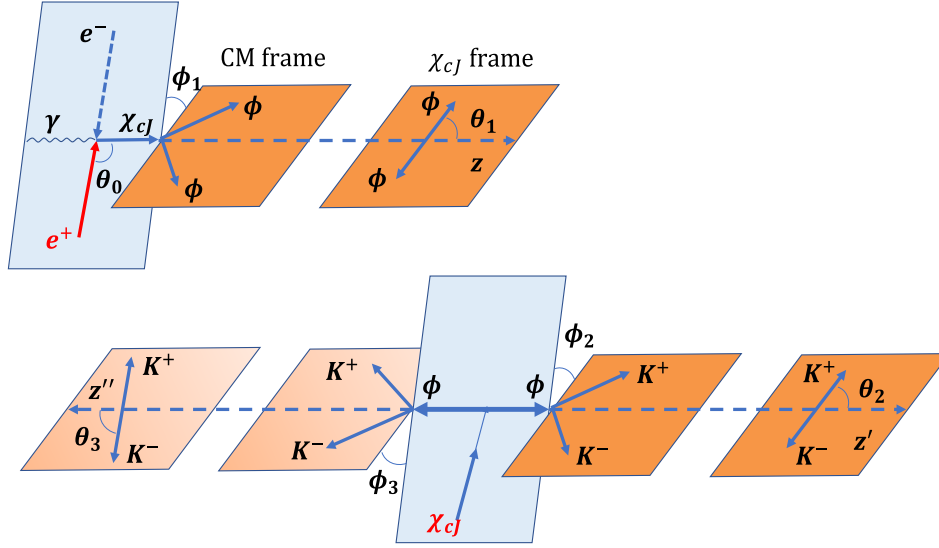


FIG. 1. Helicity system and angles definition for the $\psi(2S) \rightarrow \gamma\chi_{cJ}, \chi_{cJ} \rightarrow \phi\phi, \phi \rightarrow K^+K^-$ decay.

Here, \mathcal{I}_3 denotes a 3×3 identity matrix, and the real parameter C_{ij} is determined from the $\phi\phi$ production process, which carries polarization information for the two ϕ mesons. C_{i0} or C_{0i} means that the polarization is detected only for one ϕ meson, while C_{ij} measures the polarization correlation between two $\phi\phi$ mesons. For Q_i , we define $Q_1 = Q[1, 1, -1]$, $Q_2 = Q[1, 1, 0]$, $Q_3 = Q[1, 1, 1]$, $Q_4 = Q[1, 2, -2]$, $Q_5 = Q[1, 2, -1]$, $Q_6 = Q[1, 2, 0]$, $Q_7 = Q[1, 2, 1]$, $Q_8 = Q[1, 2, 2]$.

The polarization of $\phi\phi$ system is inaccessible in a general purpose of electromagnetic spectrometer at the modern e^+e^- colliders. Nonetheless, the subsequential decay, $\phi \rightarrow K^+K^-$, can be used as the polarimeter to measure the ϕ polarization by studying the implications of the decayed Kaon angular distribution.

We formulate the $\phi\phi \rightarrow 2(K^+K^-)$ decays with helicity amplitude method, which is defined in the helicity system as shown in Fig. 1. One ϕ decaying into K^+K^- pair is described with helicity angles (θ_2, ϕ_2) , where θ_2 is the angle spanned between the directions of K^+ and the ϕ momenta, which are defined in the rest frames of their respective mother particles. The azimuthal angle ϕ_2 is defined as the angle between the $\phi\phi$ production plane and the ϕ decay plane. The helicity angles, (θ_3, ϕ_3) , describing another ϕ meson decay, are defined by the same rule (see Table I). Then the joint angular distribution for $\phi\phi \rightarrow 2(K^+K^-)$ reads as

$$|\mathcal{M}|^2 \propto \text{Tr}[\rho_{\phi\phi} \cdot M_a \otimes M_b^\dagger] \\ = t_{00}C_{00} + \sum_{i=1}^8 (t_{i0}C_{i0} + t_{0i}C_{0i}) + \sum_{i,j=1}^8 t_{ij}C_{ij} \quad (4)$$

with

$$(M_a)_{\lambda_1, \lambda'_1} = D_{\lambda_1, 0}^{1*}(\phi_2, \theta_2, 0) D_{\lambda'_1, 0}^1(\phi_2, \theta_2, 0) f^2, \quad (5)$$

$$(M_b)_{\lambda_2, \lambda'_2} = D_{\lambda_2, 0}^{1*}(\phi_3, \theta_3, 0) D_{\lambda'_2, 0}^1(\phi_3, \theta_3, 0) f^2. \quad (6)$$

Since the helicity value f is independent on the Kaon angles, it contributes a trivial constant factor to the angular distribution. Thus, for simplicity, we can take $f^2 = 1$. The joint angular distribution can be further decomposed into the $\phi\phi$ polarization in terms of the real multipole parameters C_{ij} . The t_{ij} factors play the role of the spin observables corresponding to the parameters C_{ij} . The term t_{00} is the unpolarization cross section, while t_{0L} (t_{L0}) corresponds to the observable for detecting one ϕ polarization with rank L , and leaving another ϕ polarization being undetected. The term t_{ij} denotes the spin correlation between the two ϕ 's. Expressions of t_{ij} factors are given in terms of angles θ_i and ϕ_i ($i = 2, 3$) as shown in the Appendix A.

The multipole parameters, C_{ij} , in the $\rho_{\phi\phi}$ SDM contain the dynamical information of the $\chi_{cJ} \rightarrow \phi\phi$ decays, which can be related to the helicity amplitudes $F_{\lambda_1, \lambda_2}^{(J)}$. Thus, any theoretical prediction on their values can be tested by measuring their spin observables in experiment.

TABLE I. Definitions of helicity angles and amplitudes in the $\chi_{cJ} \rightarrow \phi\phi$ and $\phi\phi \rightarrow 2(K^+K^-)$ decays.

Decay	Angles	Amplitude
$\chi_{cJ} \rightarrow \phi(\lambda_1)\phi(\lambda_2)$	(θ_1, ϕ_1)	$F_{\lambda_1, \lambda_2}^{(J)}$
$\phi(\lambda_1) \rightarrow K^+K^-$	(θ_2, ϕ_2)	f
$\phi(\lambda_2) \rightarrow K^+K^-$	(θ_3, ϕ_3)	f

We relate the parameter C_{ij} to the helicity amplitude $F_{\lambda_1, \lambda_2}^{(J)}$ by calculating the spin density matrix $\rho_{\phi\phi}$ of the decay $\chi_{cJ} \rightarrow \phi\phi$, which reads as

$$\rho_{\phi\phi} = N \cdot \rho_J \cdot N^\dagger, \quad (7)$$

where ρ_J is a spin density matrix for χ_{cJ} with $J = 0, 1, 2$ for χ_{c0} , χ_{c1} , and χ_{c2} , respectively. N denotes decay matrix, which can be written as

$$(N)_{\lambda_1 \lambda_2 \lambda'_1 \lambda'_2, M} = D_{M, \lambda_1 - \lambda_2}^{J*}(\phi_1, \theta_1, 0) \times D_{M, \lambda'_1 - \lambda'_2}^J(\phi_1, \theta_1, 0) F_{\lambda_1, \lambda_2}^{(J)*} F_{\lambda'_1, \lambda'_2}^{(J)}, \quad (8)$$

where (θ_1, ϕ_1) are the helicity angles describing the ϕ meson flying direction as shown in Fig. 1. Azimuthal ϕ_1 is defined as the angle between the ϕ production and decay planes, while θ_1 is the angle spanned between the ϕ and χ_{cJ} momenta. $F_{\lambda_1, \lambda_2}^{(J)}$ denotes the helicity amplitude in terms of two ϕ helicity values λ_1 and λ_2 .

A special decay is $\chi_{c0} \rightarrow \phi\phi$, where the spin density matrix of χ_{c0} is reduced to Kronecker delta function, i.e., $\rho_0 = \delta_{\lambda_1, \lambda_2} \delta_{\lambda'_1, \lambda'_2}$. Then the multipole parameters C_{ij} are calculated to be

$$C_{00} = 9|F_{0,0}^{(0)}|^2 + 18|F_{1,1}^{(0)}|^2, \quad (9)$$

$$C_{44} = -\frac{3}{2}|F_{1,1}^{(0)}|^2, \quad (10)$$

$$C_{55} = -C_{77} = -\frac{3}{4}(F_{1,1}^{(0)*} F_{0,0}^{(0)} + F_{0,0}^{(0)*} F_{1,1}^{(0)}), \quad (11)$$

$$C_{60} = C_{06} = |F_{1,1}^{(0)}|^2 - |F_{0,0}^{(0)}|^2, \quad (12)$$

$$C_{66} = |F_{0,0}^{(0)}|^2 + \frac{|F_{1,1}^{(0)}|^2}{2}, \quad (13)$$

$$C_{88} = \frac{3|F_{1,1}^{(0)}|^2}{2}, \quad (14)$$

while other $C_{i,j}$ parameters are vanishing due to the spin-parity conservation in the $\chi_{c0} \rightarrow \phi\phi$ decays.

Then, with the helicity amplitude $F_{\lambda_1, \lambda_2}^{(0)}$, the ϕ angular distribution from the $\chi_{c0} \rightarrow \phi\phi$ decay can be expressed as

$$\begin{aligned} \mathcal{W}_0 \propto & \cos(\phi_{23})[4\sin^2(\theta_2)\sin^2(\theta_3)\cos(\phi_{23})|F_{1,1}^{(0)}|^2 \\ & + \sin(2\theta_2)\sin(2\theta_3)2\text{Re}(F_{1,1}^{(0)*} F_{0,0}^{(0)}) \\ & + 4\cos^2(\theta_2)\cos^2(\theta_3)|F_{0,0}^{(0)}|^2, \end{aligned} \quad (15)$$

where $\phi_{23} = \phi_2 + \phi_3$.

One can see that the ϕ angular distribution for the $\chi_{c0} \rightarrow \phi\phi$ decay is reduced to a uniform distribution either on the $\cos\theta_2(\cos\theta_3)$ or $\phi_2(\phi_3)$ observables alone. Spin correlation for $\phi\phi$ system can only be observed by measuring a moment formed by the angles θ_i and ϕ_i ($i = 2, 3$) simultaneously.

The strong decay $\chi_{c1} \rightarrow \phi\phi$ conserves the parity. Thus, the helicity amplitudes satisfy the relation $F_{-\lambda_1, -\lambda_2}^{(1)} = -F_{\lambda_1, \lambda_2}^{(1)}$, especially $F_{0,0}^{(1)} = 0$. Then the amplitudes are reduced to three independent components, i.e., $F_{1,1}^{(1)}, F_{1,0}^{(1)}$, and $F_{0,1}^{(1)}$. The matrix of helicity amplitudes is taken as

$$(F_{\lambda_1, \lambda_2}^{(1)}) = \begin{pmatrix} F_{1,1}^{(1)} & F_{1,0}^{(1)} & 0 \\ -F_{1,0}^{(1)} & 0 & -F_{0,1}^{(1)} \\ 0 & -F_{1,0}^{(1)} & -F_{1,1}^{(1)} \end{pmatrix}. \quad (16)$$

As for the χ_{c1} production from the decay $\psi(2S) \rightarrow \gamma\chi_{c1}$, its SDM is well defined and taken as $\rho_1 = \frac{1}{4}\text{diag}\{1, 2, 1\}$ [40] in its rest frame. Here, the nonvanishing parameters C_{i0} , C_{0i} , and C_{ij} are calculated and given in Appendix B.

The ϕ meson has nonzero decay width, the masses of two $\phi\phi$ may have different values from the χ_{c1} decay in a given event. However, its narrow decay width allows us to treat the $\phi\phi$ as an identical particle system statistically. Then, exchanging two ϕ mesons yields asymmetry relation $F_{1,0}^{(1)} = -F_{0,1}^{(1)}$, and $F_{1,1}^{(1)} = 0$, where the joint angular distribution is independent on the amplitude, and it reads

$$\mathcal{W}_1 \propto (2 + \sin^2\theta_1)[\cos^2\theta_2\sin^2\theta_3 + \sin^2\theta_2\cos^2\theta_3]. \quad (17)$$

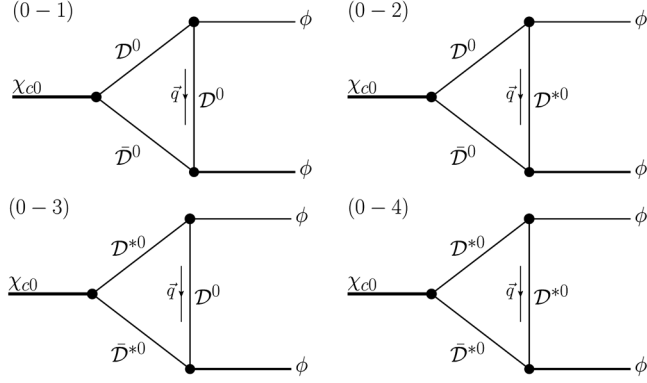
Similarly, we perform the same analysis on the $\chi_{c2} \rightarrow \phi\phi$ decay, and we take the χ_{c2} SDM as $\rho_2 = \frac{3}{20}\text{diag}\{2, 1, 2/3, 1, 2\}$ [40]. Considering the parity conservation in this decay, one has the relation $F_{-\lambda_1, -\lambda_2}^{(2)} = F_{\lambda_1, \lambda_2}^{(2)}$, then the amplitude matrix is reduced to be

$$(F_{\lambda_1, \lambda_2}^{(2)}) = \begin{pmatrix} F_{1,1}^{(2)} & F_{1,0}^{(2)} & F_{1,-1}^{(2)} \\ F_{0,1}^{(2)} & F_{0,0}^{(2)} & F_{0,1}^{(2)} \\ F_{1,-1}^{(2)} & F_{1,0}^{(2)} & F_{1,1}^{(2)} \end{pmatrix}. \quad (18)$$

With these considerations, the multipole parameters are calculated and given in Appendix C, and these expressions can be further simplified using the relation $F_{\lambda_1, \lambda_2}^{(2)} = F_{\lambda_2, \lambda_1}^{(2)}$ if one takes the $\phi\phi$ as an identical particle system.

III. MESON LOOP EFFECTS IN $\chi_{cJ} \rightarrow \phi\phi$ DECAY

Under the scenario of hadronic loop mechanism, the $\chi_{cJ} \rightarrow \phi\phi$ decays occur via the triangle loops composed of


 FIG. 2. The Feynman diagrams depicting the $\chi_{c0} \rightarrow \phi\phi$ decay via D meson loop.

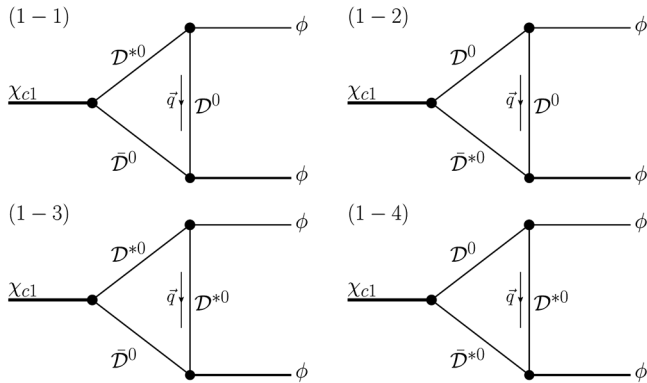
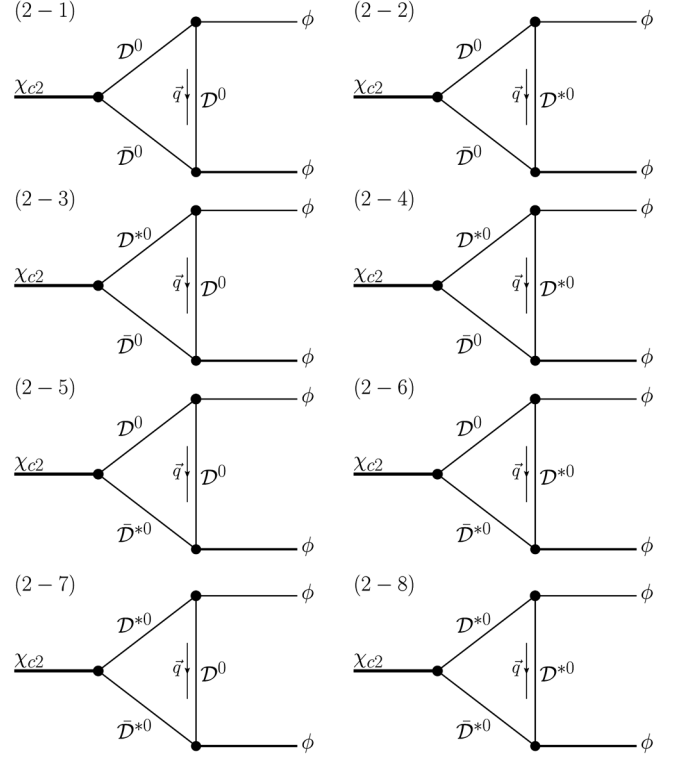
$D_{(s)}^{(*)}$ and $\bar{D}_{(s)}^{(*)}$, where these loops play the role of bridge to connect the initial χ_{cJ} and final states. In Figs. 2–4, we present the Feynman diagrams depicting the $\chi_{cJ} \rightarrow \phi\phi$ decays.

To calculate the decay amplitudes shown in Fig. 2–4, we adopt the effective Lagrangian approach; thus, at first we introduce the effective Lagrangians relevant to our calculation. For the interaction between χ_{cJ} and a pair of heavy-light mesons, the general form of the effective Lagrangian can be constructed under the chiral and heavy quark limits [42]

$$\mathcal{L}_p = ig_1 \text{Tr}[P^{(Q\bar{Q})\mu} \bar{H}^{(Qq)} \gamma_\mu \bar{H}^{(Q\bar{q})}] + \text{H.c.}, \quad (19)$$

where $P^{(Q\bar{Q})}$ and $H^{(Q\bar{q})}$ denote the P-wave multiplet of charmonia and (D, D^*) doublet, respectively. Their detailed expressions, as shown in Ref. [25,42–44], can be written as

$$P^{(Q\bar{Q})\mu} = \frac{1 + \not{p}}{2} \left[\chi_{c2}^{\mu\alpha} \gamma_\alpha + \frac{1}{\sqrt{2}} \varepsilon^{\mu\alpha\beta\gamma} v_\alpha \gamma_\beta \chi_{c1\gamma} + \frac{1}{\sqrt{3}} (\gamma^\mu - v^\mu) \chi_{c0} + h_c^\mu \gamma_5 \right] \frac{1 - \not{p}}{2}, \quad (20)$$


 FIG. 3. The Feynman diagrams depicting the $\chi_{c1} \rightarrow \phi\phi$ decay via D meson loop.

 FIG. 4. The Feynman diagrams depicting the $\chi_{c2} \rightarrow \phi\phi$ decay via D meson loop.

$$H^{(Q\bar{q})} = \frac{1 + \not{p}}{2} [D_\mu^{*0} \gamma^\mu - D \gamma^5], \quad (21)$$

respectively, with definitions $D^{(*)\dagger} = (D^{(*)+}, D^{(*)0}, D_s^{(*)0})$ and $\mathcal{D}^{(*)} = (D^{(*)-}, \bar{D}^{(*)0}, \bar{D}_s^{(*)0})^T$. $H^{(Q\bar{q})}$ corresponds to the doublet formed by homologous heavy-light antimesons, which can be obtained by applying the charge conjugation operation to $H^{(Q\bar{q})}$.

For the interaction between a light vector meson and two heavy-light mesons, the general form of the Lagrangian reads as [42,45–49]

$$\mathcal{L}_V = i\beta \text{Tr}[H^j v^\mu (-\rho_\mu)_j \bar{H}_i] + i\lambda \text{Tr}[H^j \sigma^{\mu\nu} F_{\mu\nu}(\rho) \bar{H}_i], \quad (22)$$

where

$$\rho_\mu = i \frac{g_V}{\sqrt{2}} \mathcal{V}_\mu, \quad (23)$$

$$F_{\mu\nu}(\rho) = \partial_\mu \rho_\nu - \partial_\nu \rho_\mu + [\rho_\mu, \rho_\nu], \quad (24)$$

and a vector octet \mathcal{V} has the form [22]

$$\mathcal{V} = \begin{pmatrix} \frac{\rho^0}{\sqrt{2}} + \kappa\omega^P + \zeta\phi^P & \rho^+ & K^{*+} \\ \rho^- & -\frac{\rho^0}{\sqrt{2}} + \kappa\omega^P + \zeta\phi^P & K^{*0} \\ K^{*-} & \bar{K}^{*0} & \delta\omega^P + \sigma\phi^P \end{pmatrix}, \quad (25)$$

with

$$\begin{aligned} \kappa &= \frac{\cos \theta}{\sqrt{2}}, & \zeta &= \frac{\sin \theta}{\sqrt{2}}, \\ \delta &= \sin \theta, & \sigma &= -\cos \theta. \end{aligned} \quad (26)$$

By expanding the Lagrangians in Eqs. (19) and (22), we get the following explicit forms of Lagrangians:

$$\begin{aligned} \mathcal{L}_{\chi_{cJ}\mathcal{D}^{(*)}\mathcal{D}^{(*)}} &= -g_{\chi_{c0}\mathcal{D}\mathcal{D}}\chi_{c0}\mathcal{D}\mathcal{D}^\dagger - g_{\chi_{c0}\mathcal{D}^*\mathcal{D}^*}\chi_{c0}\mathcal{D}_\mu^*\mathcal{D}^{*\mu\dagger} \\ &+ ig_{\chi_{c1}\mathcal{D}\mathcal{D}^*}\chi_{c1}^\mu(\mathcal{D}_\mu^*\mathcal{D}^\dagger - \mathcal{D}\mathcal{D}_\mu^{*\dagger}) \\ &- g_{\chi_{c2}\mathcal{D}\mathcal{D}^*}\chi_{c2}^{\mu\nu}\partial_\mu\mathcal{D}\partial_\nu\mathcal{D}^\dagger \\ &+ g_{\chi_{c2}\mathcal{D}^*\mathcal{D}^*}\chi_{c2}^{\mu\nu}(\mathcal{D}_\mu^*\mathcal{D}_\nu^{*\dagger} + \mathcal{D}_\nu^*\mathcal{D}_\mu^{*\dagger}) \\ &- ig_{\chi_{c2}\mathcal{D}^*\mathcal{D}^*}\epsilon_{\mu\alpha\beta}\partial^\alpha\chi_{c2}^{\mu\rho}(\partial_\rho\mathcal{D}^{*\nu}\partial^\beta\mathcal{D}^\dagger - \partial^\beta\mathcal{D}\partial_\rho\mathcal{D}^{*\nu\dagger}), \end{aligned} \quad (27)$$

$$\begin{aligned} \mathcal{L}_{\mathcal{D}^{(*)}\mathcal{D}^{(*)}\mathcal{V}} &= -ig_{\mathcal{D}\mathcal{D}\mathcal{V}}\mathcal{D}_i^\dagger\overleftrightarrow{\partial}^\mu\mathcal{D}^j(\mathcal{V}_\mu)_j \\ &- 2f_{\mathcal{D}^*\mathcal{D}\mathcal{V}}\epsilon_{\mu\alpha\beta}(\partial^\mu\mathcal{V}^\nu)_j(\mathcal{D}_i^\dagger\overleftrightarrow{\partial}^\alpha\mathcal{D}^{*\beta j} - \mathcal{D}_i^{*\beta\dagger}\overleftrightarrow{\partial}^\alpha\mathcal{D}^j) \\ &+ ig_{\mathcal{D}^*\mathcal{D}^*\mathcal{V}}\mathcal{D}_i^{*\nu\dagger}\overleftrightarrow{\partial}^\mu\mathcal{D}_\nu^j(\mathcal{V}_\mu)_j \\ &+ 4if_{\mathcal{D}^*\mathcal{D}^*\mathcal{V}}\mathcal{D}_{i\mu}^{*\dagger}(\partial^\mu\mathcal{V}^\nu - \partial^\nu\mathcal{V}^\mu)_j\mathcal{D}_\nu^{*j}. \end{aligned} \quad (28)$$

With these Lagrangians given in Eq. (27) and Eq. (28), the amplitudes of $\chi_{cJ} \rightarrow \phi\phi$ then can be written out. For $\chi_{c0} \rightarrow \phi\phi$ decay, with $\tilde{g}_{\mu\nu}(p) \equiv -g_{\mu\nu} + \frac{p_\mu p_\nu}{m_p^2}$, the amplitudes corresponding to Fig. 2 are

$$\begin{aligned} \mathcal{M}_{(0-1)} &= \int \frac{d^4q}{(2\pi)^4} \frac{1}{k_1^2 - m_{\mathcal{D}}^2} \frac{1}{k_2^2 - m_{\mathcal{D}}^2} \frac{1}{q^2 - m_{\mathcal{D}}^2} \mathcal{F}^2(q^2) \\ &\times [-g_{\chi_{c0}\mathcal{D}\mathcal{D}}][-g_{\mathcal{D}\mathcal{D}\phi}\epsilon_\phi^{*\zeta}(p_2)(k_{1\zeta} + q_\zeta)] \\ &\times [-g_{\mathcal{D}\mathcal{D}\phi}\epsilon_\phi^{*\lambda}(p_3)(q_\lambda - k_{2\lambda})], \end{aligned} \quad (29)$$

$$\begin{aligned} \mathcal{M}_{(0-2)} &= \int \frac{d^4q}{(2\pi)^4} \frac{1}{k_1^2 - m_{\mathcal{D}}^2} \frac{1}{k_2^2 - m_{\mathcal{D}}^2} \frac{\tilde{g}_{\xi\sigma}(q)}{q^2 - m_{\mathcal{D}^*}^2} \mathcal{F}^2(q^2) \\ &\times [-g_{\chi_{c0}\mathcal{D}\mathcal{D}}][-2f_{\mathcal{D}\mathcal{D}^*\phi}\epsilon_\phi^{*\eta\kappa\xi}\epsilon_\phi^{*\zeta}(p_2)p_{2\eta}(k_{1\kappa} + q_\kappa)] \\ &\times [2f_{\mathcal{D}\mathcal{D}^*\phi}\epsilon_\phi^{*\lambda\rho\delta\sigma}\epsilon_\phi^{*\lambda}(p_3)p_{3\rho}(q_\delta - k_{2\delta})], \end{aligned} \quad (30)$$

$$\begin{aligned} \mathcal{M}_{(0-3)} &= \int \frac{d^4q}{(2\pi)^4} \frac{\tilde{g}_\xi^\mu(k_1)}{k_1^2 - m_{\mathcal{D}^*}^2} \frac{\tilde{g}_{\mu\sigma}(k_2)}{k_2^2 - m_{\mathcal{D}^*}^2} \frac{1}{q^2 - m_{\mathcal{D}}^2} \mathcal{F}^2(q^2) \\ &\times [-g_{\chi_{c0}\mathcal{D}^*\mathcal{D}^*}][2f_{\mathcal{D}\mathcal{D}^*\phi}\epsilon_\phi^{*\eta\kappa\xi}\epsilon_\phi^{*\zeta}(p_2)p_{2\eta}(k_{1\kappa} + q_\kappa)] \\ &\times [-2f_{\mathcal{D}\mathcal{D}^*\phi}\epsilon_\phi^{*\lambda\rho\delta\sigma}\epsilon_\phi^{*\lambda}(p_3)p_{3\rho}(q_\delta - k_{2\delta})], \end{aligned} \quad (31)$$

$$\begin{aligned} \mathcal{M}_{(0-4)} &= \int \frac{d^4q}{(2\pi)^4} \frac{\tilde{g}^{\mu\psi}(k_1)}{k_1^2 - m_{\mathcal{D}^*}^2} \frac{\tilde{g}_\mu^\nu(k_2)}{k_2^2 - m_{\mathcal{D}^*}^2} \frac{\tilde{g}^{\rho\omega}(q)}{q^2 - m_{\mathcal{D}^*}^2} \mathcal{F}^2(q^2) \\ &\times [-g_{\chi_{c0}\mathcal{D}^*\mathcal{D}^*}][g_{\mathcal{D}^*\mathcal{D}^*\psi}g_{\eta\gamma}g_\psi^\eta(k_{1\zeta} + q_\zeta) \\ &- 4f_{\mathcal{D}^*\mathcal{D}^*\phi}p_2^\eta(g_{\gamma\eta}g_{\psi\zeta} - g_{\gamma\zeta}g_{\psi\eta})]\epsilon_\phi^{*\xi}(p_2) \\ &\times [g_{\mathcal{D}^*\mathcal{D}^*\phi}g_{\rho\lambda}g_\nu^\rho(q_\lambda - k_{2\lambda}) - 4f_{\mathcal{D}^*\mathcal{D}^*\phi}p_3^\lambda \\ &\times (g_{\lambda\rho}g_{\nu\lambda} - g_{\lambda\nu}g_{\rho\lambda})]\epsilon_\phi^{*\lambda}(p_3). \end{aligned} \quad (32)$$

In a similar way, the amplitudes of $\chi_{c1} \rightarrow \phi\phi$ and $\chi_{c2} \rightarrow \phi\phi$ can be written out, and are collected into Appendix D and Appendix E, respectively.

In the calculation of the $\chi_{cJ} \rightarrow \phi\phi$ amplitudes, a dipole form factor, $\mathcal{F}(q^2) = (m_E^2 - \Lambda^2)/(q^2 - \Lambda^2)^2$, is introduced to describe the structure effect and off-shell effect due to exchanging $\mathcal{D}^{(*)}$ mesons [22] at the $\mathcal{D}^{(*)}\mathcal{D}^{(*)}\phi$ and $\bar{\mathcal{D}}^{(*)}\mathcal{D}^{(*)}\phi$ vertices. This form factor plays a role similar to the Pauli-Villars renormalization scheme, which is often used to cancel the ultraviolet divergence in the loop integrals [50,51]. In the expression of $\mathcal{F}(q^2)$, m_E is the mass of the exchanged $\mathcal{D}^{(*)}$ meson and Λ denotes the cutoff, which is usually parametrized as $\Lambda = m_E + \alpha_\Lambda \Lambda_{\text{QCD}}$. Here $\Lambda_{\text{QCD}} = 0.22$ GeV; α_Λ is a free parameter [18,25–35]. Since the cutoff Λ is required to be not too far away from the physical mass of the exchanged mesons, usually α_Λ should be around 1 [35]. One notes that the multipole behavior of form factor was also suggested in the QCD sum rule study in Ref. [52]. In a series of published papers [18,25–35], this form factor was adopted in the study of transitions of charmonia, bottomonia, and B decays.

With Eqs. (29)–(32), considering charge conjugation and isospin symmetries, the polarized amplitudes of $\chi_{cJ} \rightarrow \phi\phi$ read

$$\mathcal{M}_J(i, \lambda_1, \lambda_2) = 4 \sum_j \mathcal{M}_{(J-j)}^q + 2 \sum_j \mathcal{M}_{(J-j)}^s, \quad (33)$$

where i , λ_1 , and λ_2 denote the helicities of χ_{cJ} and two ϕ mesons, respectively, $\mathcal{M}_{(J-j)}^q$ and $\mathcal{M}_{(J-j)}^s$ represent that the triangle loops are composed of charmed and charmed-strange mesons, respectively.

Thus, the helicity amplitudes can be calculated by the following expression:

$$|F_{\lambda_1, \lambda_2}^{(J)}|^2 = \sum_i \rho_J(i) |\mathcal{M}_J(i, \lambda_1, \lambda_2)|^2, \quad (34)$$

where ρ_J is the SDM given in Sec. II, i.e.,

$$\rho_0 = 1, \quad (35)$$

$$\rho_1 = \frac{1}{4} \text{diag}\{1, 2, 1\}, \quad (36)$$

$$\rho_2 = \frac{3}{20} \text{diag} \left\{ 2, 1, \frac{2}{3}, 1, 2 \right\}. \quad (37)$$

Finally, the general expression of the decay widths of $\chi_{cJ} \rightarrow \phi\phi$ decays reads as

$$\Gamma_{\chi_{cJ} \rightarrow \phi\phi} = \frac{1}{1 + \delta} \frac{1}{\sum_i \rho_J(i)} \frac{1}{8\pi m_{\chi_{cJ}}^2} \frac{|\vec{p}_\phi|}{i, \lambda_1, \lambda_2} \sum |\mathcal{M}_J(i, \lambda_1, \lambda_2)|^2, \quad (38)$$

where factor δ should be introduced if the final states are identical particles. Thus, for the discussed $\chi_{cJ} \rightarrow \phi\phi$ decays, we should take $\delta = 1$.

IV. NUMERICAL RESULTS

A. Helicity amplitudes

With the formula given in Sec. III, we estimate all the helicity amplitudes $F_{\lambda_1, \lambda_2}^{(J)}$. Besides the masses taken from the Particle Data Group (PDG) [13], other input parameters include the coupling constants, the mixing angle θ between ω^p and ϕ^p , and the parameter α_Λ that appears in the expression of form factor $\mathcal{F}(q^2)$. For the coupling constants relevant to the interactions between χ_{cJ} and $D_{(s)}^{(*)} \bar{D}_{(s)}^{(*)}$, in the heavy quark limit, they are related to one gauge coupling constant g_1 given in Eq. (19). By comparing Eq. (27) and the expanded form of Eq. (19) we can get

$$\begin{aligned} g_{\chi_{c0} \mathcal{D}\mathcal{D}} &= 2\sqrt{3}g_1 \sqrt{m_{\chi_{c0}}} m_{\mathcal{D}}, & g_{\chi_{c0} \mathcal{D}^* \mathcal{D}^*} &= \frac{2}{\sqrt{3}} g_1 \sqrt{m_{\chi_{c0}}} m_{\mathcal{D}^*}, \\ g_{\chi_{c1} \mathcal{D}\mathcal{D}^*} &= 2\sqrt{2}g_1 \sqrt{m_{\chi_{c1}}} m_{\mathcal{D}} m_{\mathcal{D}^*}, & g_{\chi_{c2} \mathcal{D}\mathcal{D}} &= 2g_1 \frac{\sqrt{m_{\chi_{c0}}}}{m_{\mathcal{D}}}, \\ g_{\chi_{c2} \mathcal{D}\mathcal{D}^*} &= g_1 \sqrt{\frac{m_{\chi_{c2}}}{m_{\mathcal{D}^*}^3 m_{\mathcal{D}}}}, & g_{\chi_{c2} \mathcal{D}^* \mathcal{D}^*} &= 4g_1 \sqrt{m_{\chi_{c2}}} m_{\mathcal{D}^*}. \end{aligned} \quad (39)$$

We determine g_1 in the following way. For the interaction between the χ_{c0} state and a pair of \mathcal{D} mesons, we define its matrix element as

$$\langle \mathcal{D}(p) \bar{\mathcal{D}}(p') | \chi_{c0}(P) \rangle = g_{\chi_{c0} \mathcal{D}\mathcal{D}}. \quad (40)$$

With the help of Isgur-Wise form factor [53,54], and the assumption that χ_{c0} gives the dominant contribution to the scalar current matrix element $\langle \mathcal{D}(p') | c\bar{c} | \mathcal{D}(p) \rangle$, together with the definition of the decay constant $f_{\chi_{c0}}$, i.e.,

$$\langle 0 | c\bar{c} | \chi_{c0}(P) \rangle = f_{\chi_{c0}} m_{\chi_{c0}}, \quad (41)$$

in $(p - p')^2$ -channel, we can express the scalar current matrix element $\langle \mathcal{D}(p') | c\bar{c} | \mathcal{D}(p) \rangle$ as

$$\begin{aligned} \langle \mathcal{D}(p') | c\bar{c} | \mathcal{D}(p) \rangle &= \frac{g_{\chi_{c0} \mathcal{D}\mathcal{D}} f_{\chi_{c0}} m_{\chi_{c0}}}{(p - p')^2 - m_{\chi_{c0}}^2} \\ &= (1 + w) \xi(w) m_{\mathcal{D}}, \end{aligned} \quad (42)$$

where $\xi(w)$ is the normalized Isgur-Wise form factor, i.e., $\xi(w = 1) = 1$ [53,54], $w = \frac{p \cdot p'}{m_{\mathcal{D}}^2}$. Thus, when $p = p'$, we have $w = 1$, then we can relate $g_{\chi_{c0} \mathcal{D}\mathcal{D}}$ to $f_{\chi_{c0}}$ as

$$g_{\mathcal{D}\mathcal{D}\chi_{c0}} = -2 \frac{m_{\mathcal{D}} m_{\chi_{c0}}}{f_{\chi_{c0}}}, \quad (43)$$

so it is easy to see that $g_1 = -\sqrt{\frac{m_{\chi_{c0}}}{3}} \frac{1}{f_{\chi_{c0}}}$, with $f_{\chi_{c0}} = 0.51$ GeV, which comes from an analysis of QCD sum rule [25,37].

For the coupling constants of $D_{(s)}^{(*)} \bar{D}_{(s)}^{(*)} \phi$ interactions, they are determined from comparison of Eq. (28) to the expansion of Eq. (22), i.e.,

$$\begin{aligned} g_{D_s, D_s \phi} &= g_{D_s^* D_s^* \phi} = \frac{\beta g_V}{\sqrt{2}} \sigma, \\ f_{D_s, D_s^* \phi} &= \frac{f_{D_s^* D_s^* \phi}}{m_{D_s^*}} = \frac{\lambda g_V}{\sqrt{2}} \sigma, \\ g_{DD\phi} &= g_{D^* D^* \phi} = \frac{\beta g_V}{\sqrt{2}} \zeta, \\ f_{DD^* \phi} &= \frac{f_{D^* D^* \phi}}{m_{D^*}} = \frac{\lambda g_V}{\sqrt{2}} \zeta, \end{aligned}$$

with $\beta = 0.9$ and $\lambda = 0.56$ GeV⁻¹. The values of β and λ come from the vector meson dominance model and the analyses of the $B \rightarrow K^* \pi$ decays, respectively [55]. Additionally, we have $g_V = m_\rho / f_\pi$ associated with the pion decay constant $f_\pi = 132$ MeV [45–48].

There still exists an undetermined parameter, i.e., the mixing angle θ between ω^p and ϕ^p . Using the Gell-Mann-Okubo mass formula [25,56,57], this parameter is roughly determined to be $\theta = 3.7^\circ$. On the other side, in the chiral perturbation theory, this mixing angle is related to the vector meson decay widths, $\Gamma(\omega \rightarrow \pi^+ \pi^-)$, $\Gamma(\rho^0 \rightarrow \pi^+ \pi^-)$, and $\Gamma(\phi \rightarrow \pi^+ \pi^-)$. Using experimental results [13], one got $\theta = (3.4 \pm 0.2)^\circ$ [57], which is consistent with $\theta = 3.7^\circ$. Thus, we set $\theta = (3.4 \pm 0.2)^\circ$ [22,57–59] in the calculation of the helicity amplitudes $F_{\lambda_1, \lambda_2}^{(J)}$.

The parameter α_Λ can be determined using the experimental data for the branching ratios of $\chi_{cJ} \rightarrow \phi\phi$ decays [13]. In our calculation, we find that if the branching ratios $\mathcal{B}(\chi_{cJ} \rightarrow \phi\phi)$ given by PDG [13] are reproduced simultaneously, α_Λ should be taken within the interval [1.15, 1.35]. The values obey the cutoff requirement, and lead to the Λ close to the physical mass of the exchanged mesons [35]. In addition, they are consistent with those in Ref. [22].

With the above parameter settings, we find that the ratios between helicity amplitudes are insensitive to the α_Λ and θ , and the ratios change a little with variations of $\alpha_\Lambda \in [1.15, 1.35]$ and $\theta = (3.4 \pm 0.2)^\circ$. We get

$$\left| \frac{F_{1,1}^{(0)}}{F_{0,0}^{(0)}} \right| = 0.359 \pm 0.019, \quad (44)$$

for the $\chi_{c0} \rightarrow \phi\phi$ decay,

$$\left| \frac{F_{1,0}^{(1)}}{F_{0,1}^{(1)}} \right| = 1, \quad \left| \frac{F_{1,1}^{(1)}}{F_{0,1}^{(1)}} \right| = 0, \quad (45)$$

for the $\chi_{c1} \rightarrow \phi\phi$ decay, and

$$\left| \frac{F_{1,0}^{(2)}}{F_{0,0}^{(2)}} \right| = \left| \frac{F_{0,1}^{(2)}}{F_{0,0}^{(2)}} \right| = 1.285 \pm 0.017, \quad (46)$$

$$\left| \frac{F_{1,-1}^{(2)}}{F_{0,0}^{(2)}} \right| = \left| \frac{F_{-1,1}^{(2)}}{F_{0,0}^{(2)}} \right| = 5.110 \pm 0.057, \quad (47)$$

$$\left| \frac{F_{-1,-1}^{(2)}}{F_{0,0}^{(2)}} \right| = \left| \frac{F_{1,1}^{(2)}}{F_{0,0}^{(2)}} \right| = 0.465 \pm 0.002, \quad (48)$$

for the $\chi_{c2} \rightarrow \phi\phi$ case.

The ratios for the χ_{c1} decays are equivalent to those determined by the parity conservation and identical particle requirement. Especially, it is interesting to note that the ratios of $F_{1,0}^{(2)}$ and $F_{1,-1}^{(2)}$ are larger than one. This indicates they receive some contributions from the long distance effects, modeled by the rescattering of charm mesons in the $\chi_{c2} \rightarrow \phi\phi$ decays. We expect the measurement available in the future and used for testing the hadron loop mechanism.

B. Polarization observables

Apart from the direct measurements on the ratios given in Sec. IV A, the t_{ij} moments, $\langle t_{ij} \rangle$, can also be selected as the spin observables, since their distributions are directly related to the helicity amplitude $F_{\lambda_1, \lambda_2}^{(J)}$. The t_{ij} observables are constructed only with the Kaon angles in ϕ decays. Thus, the $\langle t_{ij} \rangle$ moments should be independent on any parameter from theoretical investigations. In experiment, the $\langle t_{ij} \rangle$ moments are defined as

$$\langle t_{ij} \rangle = \frac{1}{I_0} \int t_{ij} |\mathcal{M}|^2 d\Omega_2 d\Omega_3, \quad (49)$$

where $|\mathcal{M}|^2$ denotes the joint angular distribution for the $\chi_{cJ} \rightarrow \phi\phi \rightarrow 2(K^+K^-)$ decay and $d\Omega_i = d\cos\theta_i d\phi_i$ ($i = 2, 3$) is the angle to be integrated out. I_0 is the normalization factor.

One exception is the $\chi_{c0} \rightarrow \phi\phi$ decay, in which the multipole parameters C_{ij} are independent on the angles of θ_1 or ϕ_1 . Thus, the $\langle t_{ij} \rangle$ moments are uniformly distributed, and they can not be used as observables. Instead, we chose an observable $\mu = \sin^2\theta_2 \sin^2\theta_3$ to express two ϕ spin entanglements produced from the χ_{c0} decays. With the joint angular distribution \mathcal{W}_0 , one has

$$\langle \mu \rangle \propto 1 + 16 |F_{1,1}^{(0)}/F_{0,0}^{(0)}|^2 \cos^2(\phi_2 + \phi_3). \quad (50)$$

An ensemble of events is generated by using the χ_{c0} decay amplitude \mathcal{W}_0 , and the ratio of amplitude is fixed to the central value of calculation, namely, $|F_{1,1}^{(0)}/F_{0,0}^{(0)}| = 0.359$. The $\langle \sin^2\theta_2 \sin^2\theta_3 \rangle$ moment of these TOY Monte Carlo (MC) events is shown in Fig. 5. One can see that the MC distribution is consistent with the expectation of $1 + 2 \cos^2(\phi_2 + \phi_3)$.

For the $\chi_{c1} \rightarrow \phi\phi$ decay, it conserves parity and the decay amplitude respects the identical particle symmetry when exchanging two ϕ mesons. Thus, the helicity amplitudes are able to factor out as an overall factor in the angular distribution. The ϕ angular distribution is independent on the amplitudes, and it is reduced to

$$\frac{dN}{d\cos\theta_1} \propto 1 - \frac{1}{3} \cos^2\theta_1, \quad (51)$$

which corresponds to the observation of moment $\langle t_{00} \rangle$ for the $\chi_{c1} \rightarrow \phi\phi$ decay.

We generate an ensemble of MC events for the χ_{c1} decay with the amplitudes constrained by the requirements of parity conservation and the identical particle symmetry, namely, $F_{1,1}^{(1)} = 0, F_{1,0}^{(1)} = -F_{0,1}^{(1)}$. Figure 6 shows the angular distribution for the ϕ meson from the χ_{c1} decays. One can see that the distribution is well consistent with the expected one as given by Eq. (51).

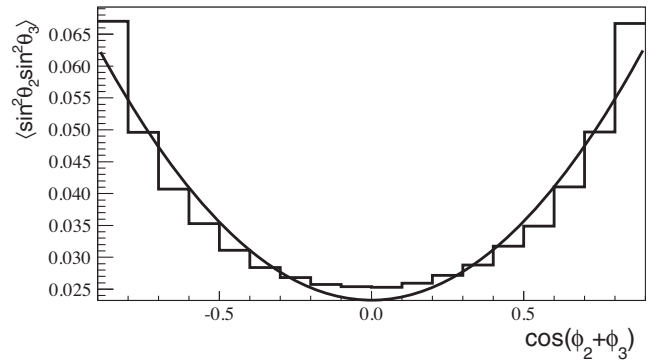


FIG. 5. Distribution of $\langle \sin^2\theta_2 \sin^2\theta_3 \rangle$ moment versus $\cos(\phi_2 + \phi_3)$ for the $\chi_{c0} \rightarrow \phi\phi \rightarrow 2(K^+K^-)$. Histogram is filled with the MC events, and the curve shows the distribution of $1 + 2 \cos^2(\phi_2 + \phi_3)$.

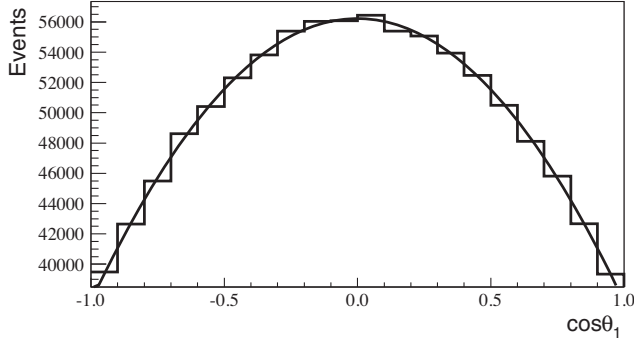


FIG. 6. Angular distribution of ϕ meson in χ_{c1} decays. Histogram is filled with the MC events, and the curve shows the distribution of $1 - \frac{1}{3}\cos^2\theta_1$.

One significant feature of t_{ij} moments for χ_{c1} decays is that their distributions are well determined only with the fundamental conservation rule and symmetry relations, being independent on the helicity amplitudes $F_{\lambda_1, \lambda_2}^{(1)}$. For example, some $\langle t_{ij} \rangle$ moments are determined to be

$$\langle t_{55} \rangle \propto 1 - \frac{1}{2}\cos^2\theta_1, \quad (52)$$

$$\langle t_{60} \rangle, \langle t_{06} \rangle, \langle t_{66} \rangle \propto 1 - \frac{1}{3}\cos^2\theta_1, \quad (53)$$

$$\langle t_{80} \rangle, \langle t_{08} \rangle, \langle t_{68} \rangle, \langle t_{86} \rangle \propto 1 - \cos^2\theta_1. \quad (54)$$

Figure 7 shows the $\langle t_{55} \rangle$ moment distribution filled with the χ_{c1} MC events. The curve shows the expected distribution, and it is well consistent with the MC events.

To show the $\langle t_{ij} \rangle$ moments for the $\chi_{c2} \rightarrow \phi\phi \rightarrow 2(K^+K^-)$ decay, we generated MC events with the central values of predicted amplitude ratios, i.e., $|F_{1,0}^{(2)}|/|F_{0,0}^{(2)}| = |F_{0,1}^{(2)}|/|F_{0,0}^{(2)}| = 1.285$, $|F_{1,-1}^{(2)}|/|F_{0,0}^{(2)}| = |F_{-1,1}^{(2)}|/|F_{0,0}^{(2)}| = 5.11$ and $|F_{1,1}^{(2)}|/|F_{0,0}^{(2)}| = 0.465$. The $\langle t_{00} \rangle$ moments corresponds to the ϕ meson angular distribution. It reads as

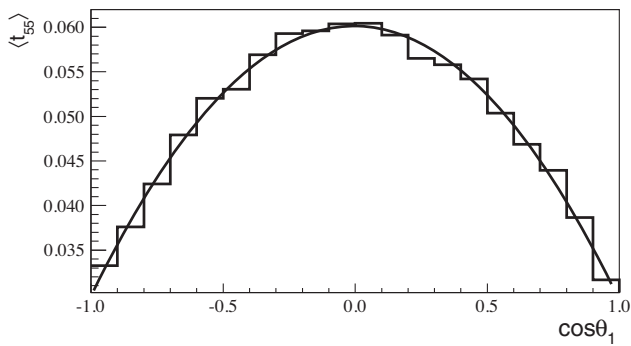


FIG. 7. Moment distribution of $\langle t_{55} \rangle$ for χ_{c1} decays. Histogram is filled with the MC events, and the curve shows the distribution of $1 - \frac{1}{2}\cos^2\theta_1$.

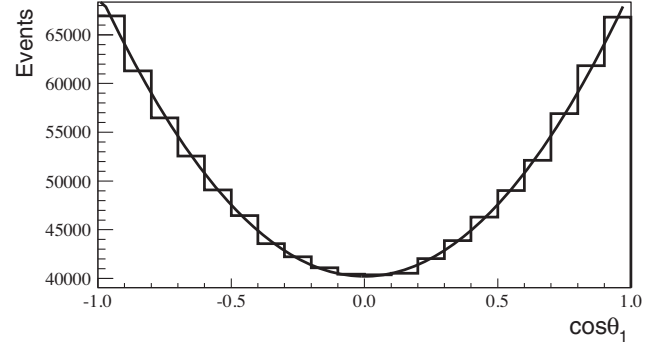


FIG. 8. Angular distribution of the ϕ meson for χ_{c2} decays. Histogram is filled with the MC events, and the curve shows the distribution of $1 + 0.736\cos^2\theta_1$.

$$\frac{dN}{d\cos\theta_1} \propto 1 + \alpha\cos^2\theta_1 \quad (55)$$

with the angular distribution parameter

$$\alpha = -\frac{3[|F_{0,0}^{(2)}|^2 + 2(-|F_{1,-1}^{(2)}|^2 + |F_{1,0}^{(2)}|^2 + |F_{1,1}^{(2)}|^2)]}{5|F_{0,0}^{(2)}|^2 + 6|F_{1,-1}^{(2)}|^2 + 18|F_{1,0}^{(2)}|^2 + 10|F_{1,1}^{(2)}|^2}. \quad (56)$$

Using the ratios, one has $\alpha = 0.736$. Figure 8 shows the angular distribution (histogram) for the ϕ meson filled with the MC events, and the comparison with the predicted angular distribution (curve).

Another moment, $\langle t_{06} \rangle$ or $\langle t_{60} \rangle$, can also be used to reveal the ratios. It distributes with the form $\langle t_{06} \rangle \propto 1 + \alpha_1\cos^2\theta_1$ with

$$\alpha_1 = -\frac{3(2|F_{0,0}^{(2)}|^2 + 2|F_{1,-1}^{(2)}|^2 + |F_{1,0}^{(2)}|^2 - 2|F_{1,1}^{(2)}|^2)}{10|F_{0,0}^{(2)}|^2 - 6|F_{1,-1}^{(2)}|^2 + 9|F_{1,0}^{(2)}|^2 - 10|F_{1,1}^{(2)}|^2}. \quad (57)$$

Using the predicted ratios, we get $\alpha_1 = 1.24$. Figure 9 shows the $\langle t_{06} \rangle$ distribution, filled with the MC events, which is comparable with the predicted distribution with $\alpha_1 = 1.24$.

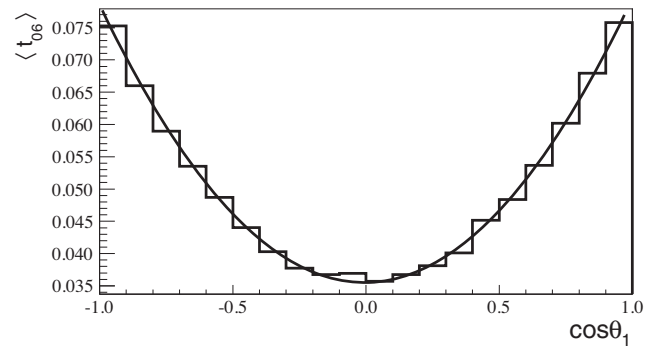


FIG. 9. Angular distribution of the ϕ meson for χ_{c2} decays. Histogram is filled with the MC events, and the curve shows the distribution of $1 + 1.26\cos^2\theta_1$.

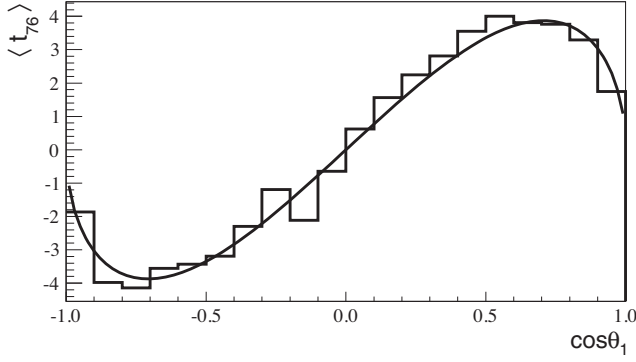


FIG. 10. Distribution of the $\langle t_{76} \rangle$ moment for χ_{c2} decays. Histogram is filled with the MC events, and the curve shows the distribution of $x\sqrt{1-x^2}$ with $x = \cos\theta_1$.

There are some $\langle t_{ij} \rangle$ moments in the χ_{c2} decays, distributing independently on the amplitude ratios. After factoring out the amplitudes, we obtain these moment distributions versus $x = \cos\theta_1$, i.e.,

$$\langle t_{44} \rangle \propto 1 - 6x^2/10, \quad (58)$$

$$\langle t_{76} \rangle, \langle t_{67} \rangle \propto x\sqrt{1-x^2}, \quad (59)$$

$$\langle t_{80} \rangle, \langle t_{08} \rangle \propto 1 - x^2. \quad (60)$$

Figure 10 shows the $\langle t_{76} \rangle$ distribution, for example, for χ_{c2} decays, and the comparison with the predicted one.

V. SUMMARY

The anomalous decay widths of the $\chi_{cJ} \rightarrow VV$ ($VV = \omega\omega, \omega\phi$ and $\phi\phi$) decays [12,15] indicate that the nonperturbative effect of strong interaction cannot be ignored. For accommodating the nonperturbative effect of strong interaction, the HLM scenario is adopted to study the branching ratios of $\chi_{cJ} \rightarrow VV$ ($VV = \omega\omega, \omega\phi$ and $\phi\phi$) decay [21,22]. Although the measured branching ratios of the $\chi_{c1} \rightarrow \omega\omega$ and $\chi_{c1} \rightarrow \phi\phi$ decays can be reproduced well, it is not the end of whole story. In this work, we are motivated to look for additional evidence to reveal the hadronic loop mechanism underlying the $\chi_{cJ} \rightarrow \phi\phi$ decays [12,15].

Inspired by Refs. [22,60–62], we propose that the analysis of polarization transfer in the $\chi_{cJ} \rightarrow VV$ decay can be applied to probe the hadronic loop mechanism, which becomes a main task of this work. One advantage of choosing the $\chi_{cJ} \rightarrow \phi\phi$ decay is due to the fact that the two ϕ decays can provide rich spin observables. Another advantage is that these decays are accessible in an experiment with high detection efficiency and two ϕ mesons can be cleanly reconstructed with low level backgrounds. High statistics allow one to perform the angular distribution analyses and get the information of the ϕ polarization,

which can shed light on the underlying decay mechanism of the $\chi_{cJ} \rightarrow VV$ decays.

In the scenario of hadronic loop mechanism, we find that the ratios of the helicity amplitudes for the $\chi_{cJ} \rightarrow \phi\phi$ decays is less dependent on the θ and α_Λ , which are the mixing angle and a free parameter in the form factor, respectively. Thus, we think that these ratios are the characteristic of HLM, and can be chosen as the observables. If they are measured in the future, the hadronic loop mechanism can be tested unambiguously.

In addition, by using the predicted amplitude ratios, we show that the observation of moments $\langle t_{ij} \rangle$ can be used to manifest the nontrivial polarization. For the χ_{c0} decays, the choice of the spin observable is quite limited due to the fact that the total spin of the $\phi\phi$ system is constrained to be zero. Thus, the spins of two ϕ mesons are antiparallel for the χ_{c0} decays. For the $\chi_{c1} \rightarrow \phi\phi$ decays, the helicity amplitudes can be well determined by considering parity conservation and the identical particle symmetry. For the $\chi_{c2} \rightarrow \phi\phi$ decays, the abundant information of the $\phi\phi$ spin configurations allows us to directly detect the helicity amplitudes from the observation of different $\langle t_{ij} \rangle$ moments. The patterns of these moments are presented based on the predicted amplitude ratios, which can be tested by experiment in the near future.

In 2019, BESIII released the white paper on its future physics program [11]. With the accumulation of charmonium data, we suggest that BESIII should pay more attention to the study of polarization of the corresponding decays, which may provide extra information for us to reveal the underlying decay mechanism of charmonia. Obviously, the present work provides a typical example and a new task for experiment.

ACKNOWLEDGMENTS

This work is supported by the National Natural Science Foundation of China under Grants No. 11875262, No. 12047501, and No. 11835012, and the China National Funds for Distinguished Young Scientists under Grant No. 11825503, National Key Research and Development Program of China under Contract No. 2020YFA0406400, the 111 Project under Grant No. B20063.

APPENDIX A: SPIN OBSERVABLE t_{ij}

The obtained spin observables t_{ij} are

$$t_{00} = \frac{1}{9},$$

$$t_{40} = -\frac{\sin^2(\theta_2) \sin(2\phi_2)}{3\sqrt{3}},$$

$$t_{04} = -\frac{\sin^2(\theta_3) \sin(2\phi_3)}{3\sqrt{3}},$$

$$t_{44} = \frac{1}{3} \sin^2(\theta_2) \sin^2(\theta_3) \sin(2\phi_2) \sin(2\phi_3),$$

$$\begin{aligned}
t_{45} &= \frac{1}{3} \sin^2(\theta_2) \sin(2\theta_3) \sin(2\phi_2) \sin(\phi_3), \\
t_{46} &= \frac{\sin^2(\theta_2)(3 \cos(2\theta_3) + 1) \sin(2\phi_2)}{6\sqrt{3}}, \\
t_{47} &= \frac{1}{3} \sin^2(\theta_2) \sin(2\theta_3) \sin(2\phi_2) \cos(\phi_3), \\
t_{48} &= \frac{1}{3} \sin^2(\theta_2) \sin^2(\theta_3) \sin(2\phi_2) \cos(2\phi_3), \\
t_{50} &= -\frac{\sin(2\theta_2) \sin(\phi_2)}{3\sqrt{3}}, \\
t_{51} &= -\frac{\sin(2\theta_3) \sin(\phi_3)}{3\sqrt{3}}, \\
t_{54} &= \frac{1}{3} \sin(2\theta_2) \sin^2(\theta_3) \sin(\phi_2) \sin(2\phi_3), \\
t_{55} &= \frac{1}{3} \sin(2\theta_2) \sin(2\theta_3) \sin(\phi_2) \sin(\phi_3), \\
t_{56} &= \frac{\sin(2\theta_2)(3 \cos(2\theta_3) + 1) \sin(\phi_2)}{6\sqrt{3}}, \\
t_{57} &= \frac{1}{3} \sin(2\theta_2) \sin(2\theta_3) \sin(\phi_2) \cos(\phi_3), \\
t_{58} &= \frac{1}{3} \sin(2\theta_2) \sin^2(\theta_3) \sin(\phi_2) \cos(2\phi_3), \\
t_{60} &= \frac{1}{18} (-3 \cos(2\theta_2) - 1), \\
t_{61} &= \frac{1}{18} (-3 \cos(2\theta_3) - 1), \\
t_{64} &= \frac{\sin^2(\theta_3)(3 \cos(2\theta_2) + 1) \sin(2\phi_3)}{6\sqrt{3}}, \\
t_{65} &= \frac{\sin(2\theta_3)(3 \cos(2\theta_2) + 1) \sin(\phi_3)}{6\sqrt{3}}, \\
t_{66} &= \frac{1}{36} (3 \cos(2\theta_2) + 1)(3 \cos(2\theta_3) + 1), \\
t_{67} &= \frac{\sin(2\theta_3)(3 \cos(2\theta_2) + 1) \cos(\phi_3)}{6\sqrt{3}}, \\
t_{68} &= \frac{\sin^2(\theta_3)(3 \cos(2\theta_2) + 1) \cos(2\phi_3)}{6\sqrt{3}}, \\
t_{70} &= -\frac{\sin(2\theta_2) \cos(\phi_2)}{3\sqrt{3}}, \\
t_{71} &= -\frac{\sin(2\theta_3) \cos(\phi_3)}{3\sqrt{3}}, \\
t_{74} &= \frac{1}{3} \sin(2\theta_2) \sin^2(\theta_3) \sin(2\phi_3) \cos(\phi_2), \\
t_{75} &= \frac{1}{3} \sin(2\theta_2) \sin(2\theta_3) \sin(\phi_3) \cos(\phi_2), \\
t_{76} &= \frac{\sin(2\theta_2)(3 \cos(2\theta_3) + 1) \cos(\phi_2)}{6\sqrt{3}}, \\
t_{77} &= \frac{1}{3} \sin(2\theta_2) \sin(2\theta_3) \cos(\phi_2) \cos(\phi_3),
\end{aligned}$$

$$\begin{aligned}
t_{78} &= \frac{1}{3} \sin(2\theta_2) \sin^2(\theta_3) \cos(\phi_2) \cos(2\phi_3), \\
t_{80} &= -\frac{\sin^2(\theta_2) \cos(2\phi_2)}{3\sqrt{3}}, \\
t_{81} &= -\frac{\sin^2(\theta_3) \cos(2\phi_3)}{3\sqrt{3}}, \\
t_{84} &= \frac{1}{3} \sin^2(\theta_2) \sin^2(\theta_3) \sin(2\phi_3) \cos(2\phi_2), \\
t_{85} &= \frac{1}{3} \sin^2(\theta_2) \sin(2\theta_3) \sin(\phi_3) \cos(2\phi_2), \\
t_{86} &= \frac{\sin^2(\theta_2)(3 \cos(2\theta_3) + 1) \cos(2\phi_2)}{6\sqrt{3}}, \\
t_{87} &= \frac{1}{3} \sin^2(\theta_2) \sin(2\theta_3) \cos(2\phi_2) \cos(\phi_3), \\
t_{88} &= \frac{1}{3} \sin^2(\theta_2) \sin^2(\theta_3) \cos(2\phi_2) \cos(2\phi_3).
\end{aligned}$$

APPENDIX B: MULTIPOLE PARAMETERS FOR $\chi_{c1} \rightarrow \phi\phi$

We collected the multipole parameters for $\chi_{c1} \rightarrow \phi\phi$, i.e.,

$$\begin{aligned}
C_{00} &= \frac{9}{8} (-\cos(2\theta_1) - 5) |F_{0,1}^{(1)}|^2 \\
&\quad - (\cos(2\theta_1) - 5) |F_{1,0}^{(1)}|^2 + 2(\cos(2\theta_1) + 3) |F_{1,1}^{(1)}|^2, \\
C_{54} &= \frac{3}{32} \sin(2\theta_1) (F_{1,1}^{(1)*} F_{0,1}^{(1)} + F_{0,1}^{(1)*} F_{1,1}^{(1)}), \\
C_{55} &= \frac{3}{32} (\cos(2\theta_1) - 3) (F_{1,0}^{(1)*} F_{0,1}^{(1)} + F_{0,1}^{(1)*} F_{1,0}^{(1)}), \\
C_{60} &= \frac{1}{16} (2(\cos(2\theta_1) - 5) |F_{0,1}^{(1)}|^2 - (\cos(2\theta_1) - 5) |F_{1,0}^{(1)}|^2 \\
&\quad + 2(\cos(2\theta_1) + 3) |F_{1,1}^{(1)}|^2), \\
C_{06} &= \frac{1}{16} (2((\cos(2\theta_1) - 5) |F_{1,0}^{(1)}|^2 + (\cos(2\theta_1) + 3) |F_{1,1}^{(1)}|^2) \\
&\quad - (\cos(2\theta_1) - 5) |F_{0,1}^{(1)}|^2), \\
C_{66} &= \frac{1}{16} ((\cos(2\theta_1) - 5) |F_{0,1}^{(1)}|^2 + (\cos(2\theta_1) - 5) |F_{1,0}^{(1)}|^2 \\
&\quad + (\cos(2\theta_1) + 3) |F_{1,1}^{(1)}|^2), \\
C_{67} &= \frac{1}{32} \sqrt{3} \sin(2\theta_1) (F_{1,1}^{(1)*} F_{1,0}^{(1)} + F_{1,0}^{(1)*} F_{1,1}^{(1)}), \\
C_{68} &= -\frac{1}{8} \sqrt{3} \sin^2(\theta_1) |F_{0,1}^{(1)}|^2, \\
C_{70} &= -\frac{1}{16} \sqrt{3} \sin(2\theta_1) (F_{1,1}^{(1)*} F_{0,1}^{(1)} + F_{0,1}^{(1)*} F_{1,1}^{(1)}), \\
C_{07} &= \frac{1}{16} \sqrt{3} \sin(2\theta_1) (F_{1,1}^{(1)*} F_{1,0}^{(1)} + F_{1,0}^{(1)*} F_{1,1}^{(1)}), \\
C_{76} &= -\frac{1}{32} \sqrt{3} \sin(2\theta_1) (F_{1,1}^{(1)*} F_{0,1}^{(1)} + F_{0,1}^{(1)*} F_{1,1}^{(1)}),
\end{aligned}$$

$$\begin{aligned}
 C_{77} &= \frac{3}{16} (F_{1,0}^{(1)*} F_{0,1}^{(1)} + F_{0,1}^{(1)*} F_{1,0}^{(1)}), \\
 C_{78} &= -\frac{3}{32} \sin(2\theta_1) (F_{1,1}^{(1)*} F_{0,1}^{(1)} + F_{0,1}^{(1)*} F_{1,1}^{(1)}), \\
 C_{80} &= \frac{1}{8} \sqrt{3} \sin^2(\theta_1) |F_{1,0}^{(1)}|^2, \\
 C_{08} &= \frac{1}{8} \sqrt{3} \sin^2(\theta_1) |F_{0,1}^{(1)}|^2, \\
 C_{86} &= -\frac{1}{8} \sqrt{3} \sin^2(\theta_1) |F_{1,0}^{(1)}|^2, \\
 C_{87} &= \frac{3}{32} \sin(2\theta_1) (F_{1,1}^{(1)*} F_{1,0}^{(1)} + F_{1,0}^{(1)*} F_{1,1}^{(1)}), \\
 C_{88} &= -\frac{3}{16} (\cos(2\theta_1) + 3) |F_{1,1}^{(1)}|^2.
 \end{aligned}$$

APPENDIX C: MULTIPOLE PARAMETERS FOR $\chi_{c2} \rightarrow \phi\phi$

The multipole parameters for $\chi_{c2} \rightarrow \phi\phi$ are

$$\begin{aligned}
 C_{00} &= \frac{9}{40} [-3 \cos(2\theta_1) \\
 &\quad \times (|F_{1,0}^{(2)}|^2 + 2|F_{1,1}^{(2)}|^2 + F_{1,0}^{(2)*} F_{0,1}^{(2)} - F_{-1,1}^{(2)*} F_{1,-1}^{(2)}) \\
 &\quad + (7 - 3 \cos(2\theta_1)) |F_{0,0}^{(2)}|^2 + 3(\cos(2\theta_1) + 3) |F_{1,-1}^{(2)}|^2 \\
 &\quad + 15|F_{1,0}^{(2)}|^2 + 14|F_{1,1}^{(2)}|^2 + 15F_{1,0}^{(2)*} F_{0,1}^{(2)} + 9F_{-1,1}^{(2)*} F_{1,-1}^{(2)}], \\
 C_{44} &= \frac{3}{80} (3 \cos(2\theta_1) - 7) |F_{1,1}^{(2)}|^2, \\
 C_{45} &= -\frac{3}{160} \sqrt{3} \sin(2\theta_1) (F_{1,1}^{(2)*} F_{1,0}^{(2)} + F_{1,0}^{(2)*} F_{1,1}^{(2)}), \\
 C_{54} &= \frac{3}{160} \sqrt{3} \sin(2\theta_1) (F_{1,1}^{(2)*} F_{1,0}^{(2)} + F_{1,0}^{(2)*} F_{1,1}^{(2)}), \\
 C_{55} &= -\frac{3}{160} (6(\cos(2\theta_1) - 3) |F_{1,0}^{(2)}|^2 \\
 &\quad + \sqrt{6} \sin^2(\theta_1) (F_{1,-1}^{(2)*} F_{0,0}^{(2)} + F_{0,0}^{(2)*} F_{1,-1}^{(2)}) \\
 &\quad - (3 \cos(2\theta_1) - 7) (F_{1,1}^{(2)*} F_{0,0}^{(2)} + F_{0,0}^{(2)*} F_{1,1}^{(2)})), \quad (C1) \\
 C_{60} &= \frac{1}{40} ((3 \cos(2\theta_1) - 7) |F_{0,0}^{(2)}|^2 + (7 - 3 \cos(2\theta_1)) |F_{1,1}^{(2)}|^2 \\
 &\quad + 3(\cos(2\theta_1) + 3) |F_{1,-1}^{(2)}|^2), \\
 C_{06} &= \frac{1}{40} ((3 \cos(2\theta_1) - 7) |F_{0,0}^{(2)}|^2 + (7 - 3 \cos(2\theta_1)) |F_{1,1}^{(2)}|^2 \\
 &\quad + 3(\cos(2\theta_1) + 3) |F_{1,-1}^{(2)}|^2), \quad (C2) \\
 C_{66} &= \frac{1}{80} (2(7 - 3 \cos(2\theta_1)) |F_{0,0}^{(2)}|^2 + (7 - 3 \cos(2\theta_1)) |F_{1,1}^{(2)}|^2 \\
 &\quad + 6(\cos(2\theta_1) - 5) |F_{1,0}^{(2)}|^2 \\
 &\quad + 3(\cos(2\theta_1) + 3) |F_{1,-1}^{(2)}|^2),
 \end{aligned}$$

$$\begin{aligned}
 C_{67} &= -\frac{3}{160} \sin(2\theta_1) ((2F_{0,0}^{(2)*} - \sqrt{6}F_{1,-1}^{(2)*} + F_{1,1}^{(2)*}) F_{1,0}^{(2)} \\
 &\quad + F_{1,0}^{(2)*} (2F_{0,0}^{(2)} - \sqrt{6}F_{1,-1}^{(2)} + F_{1,1}^{(2)})), \\
 C_{68} &= \frac{3}{80} \sin^2(\theta_1) (\sqrt{2} (F_{1,1}^{(2)*} F_{1,-1}^{(2)} + F_{1,-1}^{(2)*} F_{1,1}^{(2)}) \\
 &\quad - 2\sqrt{3} |F_{1,0}^{(2)}|^2), \\
 C_{76} &= \frac{3}{160} \sin(2\theta_1) ((2F_{0,0}^{(2)*} - \sqrt{6}F_{1,-1}^{(2)*} + F_{1,1}^{(2)*}) F_{1,0}^{(2)} \\
 &\quad + F_{1,0}^{(2)*} (2F_{0,0}^{(2)} - \sqrt{6}F_{1,-1}^{(2)} + F_{1,1}^{(2)})), \\
 C_{77} &= -\frac{3}{160} (12|F_{1,0}^{(2)}|^2 \\
 &\quad + \sqrt{6} \sin^2(\theta_1) (F_{1,-1}^{(2)*} F_{0,0}^{(2)} + F_{0,0}^{(2)*} F_{1,-1}^{(2)}) \\
 &\quad + (3 \cos(2\theta_1) - 7) (F_{1,1}^{(2)*} F_{0,0}^{(2)} + F_{0,0}^{(2)*} F_{1,1}^{(2)})), \\
 C_{78} &= -\frac{3}{160} \sqrt{3} \sin(2\theta_1) (F_{1,1}^{(2)*} F_{1,0}^{(2)} + F_{1,0}^{(2)*} F_{1,1}^{(2)}), \\
 C_{80} &= \frac{3 \sin^2(\theta_1) (F_{1,1}^{(2)*} F_{1,-1}^{(2)} + F_{1,-1}^{(2)*} F_{1,1}^{(2)})}{20\sqrt{2}}, \\
 C_{08} &= \frac{3 \sin^2(\theta_1) (F_{1,1}^{(2)*} F_{1,-1}^{(2)} + F_{1,-1}^{(2)*} F_{1,1}^{(2)})}{20\sqrt{2}}, \\
 C_{86} &= \frac{3}{80} \sin^2(\theta_1) (\sqrt{2} (F_{1,1}^{(2)*} F_{1,-1}^{(2)} + F_{1,-1}^{(2)*} F_{1,1}^{(2)}) \\
 &\quad - 2\sqrt{3} |F_{1,0}^{(2)}|^2), \\
 C_{87} &= \frac{3}{160} \sqrt{3} \sin(2\theta_1) (F_{1,1}^{(2)*} F_{1,0}^{(2)} + F_{1,0}^{(2)*} F_{1,1}^{(2)}), \\
 C_{88} &= -\frac{3}{80} (3 \cos(2\theta_1) - 7) |F_{1,1}^{(2)}|^2.
 \end{aligned}$$

APPENDIX D: AMPLITUDES OF $\chi_{c1} \rightarrow \phi\phi$ DECAY

For $\chi_{c1} \rightarrow \phi\phi$ decay, the amplitudes corresponding to Fig. 3 are

$$\begin{aligned}
 \mathcal{M}_{(1-1)} &= \int \frac{d^4 q}{(2\pi)^4} \frac{\tilde{g}_\xi^\mu(k_1)}{k_1^2 - m_{\mathcal{D}^*}^2} \frac{1}{k_2^2 - m_{\mathcal{D}^*}^2} \frac{1}{q^2 - m_{\mathcal{D}}^2} \mathcal{F}^2(q^2) \\
 &\quad \times [-ig_{\chi_{c1} \mathcal{D} \mathcal{D}^*} \epsilon_{\chi_{c1}}^\mu(p_1)] [-g_{\mathcal{D} \mathcal{D} \phi} \epsilon_\phi^{*\lambda}(p_3) (q_\lambda - k_{2\lambda})] \\
 &\quad \times [2f_{\mathcal{D} \mathcal{D}^* \phi} \epsilon^{\xi \eta \kappa \xi} \epsilon_\phi^{*\zeta}(p_2) p_{2\eta} (k_{1\kappa} + q_\kappa)], \quad (D1)
 \end{aligned}$$

$$\begin{aligned}
 \mathcal{M}_{(1-2)} &= \int \frac{d^4 q}{(2\pi)^4} \frac{1}{k_1^2 - m_{\mathcal{D}}^2} \frac{\tilde{g}_{\sigma\mu}(k_2)}{k_2^2 - m_{\mathcal{D}^*}^2} \frac{1}{q^2 - m_{\mathcal{D}}^2} \mathcal{F}^2(q^2) \\
 &\quad \times [ig_{\chi_{c1} \mathcal{D} \mathcal{D}^*} \epsilon_{\chi_{c1}}^\mu(p_1)] [-g_{\mathcal{D} \mathcal{D} \phi} \epsilon_\phi^{*\zeta}(p_2) (k_{1\xi} + q_\xi)] \\
 &\quad \times [-2f_{\mathcal{D} \mathcal{D}^* \phi} \epsilon^{\lambda\rho\delta\sigma} \epsilon_{\phi\lambda}^*(p_3) p_{3\rho} (q_\delta - k_{2\delta})], \quad (D2)
 \end{aligned}$$

$$\begin{aligned}
\mathcal{M}_{(1-3)} = & \int \frac{d^4 q}{(2\pi)^4} \frac{\tilde{g}^{\mu\nu}(k_1)}{k_1^2 - m_{\mathcal{D}}^2} \frac{1}{k_2^2 - m_{\mathcal{D}}^2} \frac{\tilde{g}'_\sigma(q)}{q^2 - m_{\mathcal{D}^*}^2} \mathcal{F}^2(q^2) \\
& \times [-ig_{\chi_{c1} \mathcal{D} \mathcal{D}^*} \epsilon_{\chi_{c1}}^\mu(p_1)] [g_{\mathcal{D}^* \mathcal{D}^* \psi} g_{\eta\gamma} g_{\psi\eta}^\eta(k_{1\zeta} + q_\zeta) \\
& - 4f_{\mathcal{D}^* \mathcal{D}^* \phi} p_2^\eta (g_{\gamma\eta} g_{\psi\zeta} - g_{\gamma\zeta} g_{\psi\eta})] \epsilon_\phi^{*\zeta}(p_2) \\
& \times [2f_{\mathcal{D} \mathcal{D}^* \phi} \epsilon^{\lambda\rho\delta\sigma} \epsilon_{\phi\lambda}^*(p_3) p_{3\rho} (q_\delta - k_{2\delta})], \quad (\text{D3})
\end{aligned}$$

$$\begin{aligned}
\mathcal{M}_{(1-4)} = & \int \frac{d^4 q}{(2\pi)^4} \frac{1}{k_1^2 - m_{\mathcal{D}}^2} \frac{\tilde{g}^{\mu\nu}(k_2)}{k_2^2 - m_{\mathcal{D}}^2} \frac{\tilde{g}'_\xi(q)}{q^2 - m_{\mathcal{D}^*}^2} \mathcal{F}^2(q^2) \\
& \times [-2f_{\mathcal{D} \mathcal{D}^* \phi} \epsilon^{\zeta\eta\kappa\xi} \epsilon_{\phi\zeta}^*(p_2) p_{2\eta} (k_{1\kappa} + q_\kappa)] \\
& \times \epsilon_\phi^{*\lambda}(p_3) [g_{\mathcal{D}^* \mathcal{D}^* \phi} g_{\rho\lambda} g_{\nu}^\rho (q_\lambda - k_{2\lambda}) \\
& - 4f_{\mathcal{D}^* \mathcal{D}^* \phi} p_3^\rho (g_{\rho\nu} g_{\nu\lambda} - g_{\rho\lambda} g_{\nu\rho})] \\
& \times [ig_{\chi_{c1} \mathcal{D} \mathcal{D}^*} \epsilon_{\chi_{c1}}^\mu(p_1)]. \quad (\text{D4})
\end{aligned}$$

APPENDIX E: AMPLITUDES OF $\chi_{c2} \rightarrow \phi\phi$ DECAY

The obtained amplitudes of the $\chi_{c2} \rightarrow \phi\phi$ decay for Fig. 4 are

$$\begin{aligned}
\mathcal{M}_{(2-1)} = & \int \frac{d^4 q}{(2\pi)^4} \frac{1}{k_1^2 - m_{\mathcal{D}}^2} \frac{1}{k_2^2 - m_{\mathcal{D}}^2} \frac{1}{q^2 - m_{\mathcal{D}^*}^2} \mathcal{F}^2(q^2) \\
& \times [g_{\chi_{c2} \mathcal{D} \mathcal{D}^*} \epsilon_{\chi_{c2}}^{\mu\nu}(p_1) k_{2\mu} k_{1\nu}] \\
& \times [g_{\mathcal{D} \mathcal{D} \phi} \epsilon_\phi^{*\zeta}(p_2) (k_{1\zeta} + q_\zeta)] \\
& \times [g_{\mathcal{D} \mathcal{D} \phi} \epsilon_\phi^{*\lambda}(p_3) (q_\lambda - k_{2\lambda})], \quad (\text{E1})
\end{aligned}$$

$$\begin{aligned}
\mathcal{M}_{(2-2)} = & \int \frac{d^4 q}{(2\pi)^4} \frac{\tilde{g}'_\xi(k_1)}{k_1^2 - m_{\mathcal{D}^*}^2} \frac{1}{k_2^2 - m_{\mathcal{D}}^2} \frac{1}{q^2 - m_{\mathcal{D}}^2} \mathcal{F}^2(q^2) \\
& \times [-g_{\chi_{c2} \mathcal{D} \mathcal{D}^*} \epsilon_{\mu\tau\alpha\beta} p_1^\alpha \epsilon_{\chi_{c2}}^{\mu\nu}(p_1) k_{2\nu} k_{1\tau}] \\
& \times [2f_{\mathcal{D} \mathcal{D}^* \phi} \epsilon^{\zeta\eta\kappa\xi} \epsilon_{\phi\zeta}^*(p_2) p_{2\eta} (k_{1\kappa} + q_\kappa)] \\
& \times [-g_{\mathcal{D} \mathcal{D} \phi} \epsilon_\phi^{*\lambda}(p_3) (q_\lambda - k_{2\lambda})], \quad (\text{E2})
\end{aligned}$$

$$\begin{aligned}
\mathcal{M}_{(2-3)} = & \int \frac{d^4 q}{(2\pi)^4} \frac{1}{k_1^2 - m_{\mathcal{D}}^2} \frac{\tilde{g}'_\sigma(k_2)}{k_2^2 - m_{\mathcal{D}^*}^2} \frac{1}{q^2 - m_{\mathcal{D}}^2} \mathcal{F}^2(q^2) \\
& \times [-g_{\chi_{c2} \mathcal{D} \mathcal{D}^*} \epsilon_{\mu\tau\alpha\beta} p_1^\alpha \epsilon_{\chi_{c2}}^{\mu\nu}(p_1) k_{2\nu} k_{1\tau}] \\
& \times [-g_{\mathcal{D} \mathcal{D} \phi} \epsilon_\phi^{*\zeta}(p_2) (k_{1\zeta} + q_\zeta)] \\
& \times [-2f_{\mathcal{D} \mathcal{D}^* \phi} \epsilon^{\lambda\rho\delta\sigma} \epsilon_{\phi\lambda}^*(p_3) p_{3\rho} (q_\delta - k_{2\delta})], \quad (\text{E3})
\end{aligned}$$

$$\begin{aligned}
\mathcal{M}_{(2-4)} = & \int \frac{d^4 q}{(2\pi)^4} \frac{1}{k_1^2 - m_{\mathcal{D}}^2} \frac{1}{k_2^2 - m_{\mathcal{D}}^2} \frac{\tilde{g}'_{\xi\sigma}(q)}{q^2 - m_{\mathcal{D}^*}^2} \mathcal{F}^2(q^2) \\
& \times [g_{\chi_{c2} \mathcal{D} \mathcal{D}^*} \epsilon_{\chi_{c2}}^{\mu\nu}(p_1) k_{2\mu} k_{1\nu}] \\
& \times [-2f_{\mathcal{D} \mathcal{D}^* \phi} \epsilon^{\zeta\eta\kappa\xi} \epsilon_{\phi\zeta}^*(p_2) p_{2\eta} (k_{1\kappa} + q_\kappa)] \\
& \times [2f_{\mathcal{D} \mathcal{D}^* \phi} \epsilon^{\lambda\rho\delta\sigma} \epsilon_{\phi\lambda}^*(p_3) p_{3\rho} (q_\delta - k_{2\delta})], \quad (\text{E4})
\end{aligned}$$

$$\begin{aligned}
\mathcal{M}_{(2-5)} = & \int \frac{d^4 q}{(2\pi)^4} \frac{\tilde{g}_{\omega\xi}(k_1)}{k_1^2 - m_{\mathcal{D}}^2} \frac{\tilde{g}_{\chi\sigma}(k_2)}{k_2^2 - m_{\mathcal{D}}^2} \frac{1}{q^2 - m_{\mathcal{D}}^2} \mathcal{F}^2(q^2) \\
& \times [g_{\chi_{c2} \mathcal{D}^* \mathcal{D}^*} \epsilon_{\chi_{c2}}^{\mu\nu}(p_1) (g_{\nu\omega} g_{\mu\chi} + g_{\mu\omega} g_{\nu\chi})] \\
& \times [2f_{\mathcal{D} \mathcal{D}^* \phi} \epsilon^{\zeta\eta\kappa\xi} \epsilon_{\phi\zeta}^*(p_2) p_{2\eta} (k_{1\kappa} + q_\kappa)] \\
& \times [-2f_{\mathcal{D} \mathcal{D}^* \phi} \epsilon^{\lambda\rho\delta\sigma} \epsilon_{\phi\lambda}^*(p_3) p_{3\rho} (q_\delta - k_{2\delta})], \quad (\text{E5})
\end{aligned}$$

$$\begin{aligned}
\mathcal{M}_{(2-6)} = & \int \frac{d^4 q}{(2\pi)^4} \frac{\tilde{g}^{\tau\nu}(k_1)}{k_1^2 - m_{\mathcal{D}}^2} \frac{1}{k_2^2 - m_{\mathcal{D}}^2} \frac{\tilde{g}'_\sigma(q)}{q^2 - m_{\mathcal{D}^*}^2} \mathcal{F}^2(q^2) \\
& \times [-g_{\chi_{c2} \mathcal{D} \mathcal{D}^*} \epsilon_{\mu\tau\alpha\beta} p_1^\alpha \epsilon_{\chi_{c2}}^{\mu\nu}(p_1) k_{2\nu} k_{1\tau}] \\
& \times \epsilon_\phi^{*\zeta}(p_2) [g_{\mathcal{D}^* \mathcal{D}^* \psi} g_{\eta\gamma} g_{\psi\eta}^\eta(k_{1\zeta} + q_\zeta) \\
& - 4f_{\mathcal{D}^* \mathcal{D}^* \phi} p_2^\eta (g_{\gamma\eta} g_{\psi\zeta} - g_{\gamma\zeta} g_{\psi\eta})] \\
& \times [2f_{\mathcal{D} \mathcal{D}^* \phi} \epsilon^{\lambda\rho\delta\sigma} \epsilon_{\phi\lambda}^*(p_3) p_{3\rho} (q_\delta - k_{2\delta})], \quad (\text{E6})
\end{aligned}$$

$$\begin{aligned}
\mathcal{M}_{(2-7)} = & \int \frac{d^4 q}{(2\pi)^4} \frac{1}{k_1^2 - m_{\mathcal{D}}^2} \frac{\tilde{g}'^{\tau\nu}(k_2)}{k_2^2 - m_{\mathcal{D}^*}^2} \frac{\tilde{g}'_\xi(q)}{q^2 - m_{\mathcal{D}^*}^2} \mathcal{F}^2(q^2) \\
& \times [-g_{\chi_{c2} \mathcal{D} \mathcal{D}^*} \epsilon_{\mu\tau\alpha\beta} p_1^\alpha \epsilon_{\chi_{c2}}^{\mu\nu}(p_1) k_{2\nu} k_{1\tau}] \\
& \times [-2f_{\mathcal{D} \mathcal{D}^* \phi} \epsilon^{\zeta\eta\kappa\xi} \epsilon_{\phi\zeta}^*(p_2) p_{2\eta} (k_{1\kappa} + q_\kappa)] \\
& \times \epsilon_\phi^{*\lambda}(p_3) [g_{\mathcal{D}^* \mathcal{D}^* \phi} g_{\rho\lambda} g_{\nu}^\rho (q_\lambda - k_{2\lambda}) \\
& - 4f_{\mathcal{D}^* \mathcal{D}^* \phi} p_3^\rho (g_{\rho\nu} g_{\nu\lambda} - g_{\rho\lambda} g_{\nu\rho})], \quad (\text{E7})
\end{aligned}$$

$$\begin{aligned}
\mathcal{M}_{(2-8)} = & \int \frac{d^4 q}{(2\pi)^4} \frac{\tilde{g}'_\omega(k_1)}{k_1^2 - m_{\mathcal{D}}^2} \frac{\tilde{g}'_\chi(k_2)}{k_2^2 - m_{\mathcal{D}}^2} \frac{\tilde{g}'^{\nu\sigma}(q)}{q^2 - m_{\mathcal{D}^*}^2} \mathcal{F}^2(q^2) \\
& \times [g_{\chi_{c2} \mathcal{D}^* \mathcal{D}^*} \epsilon_{\chi_{c2}}^{\mu\nu}(p_1) (g_{\nu\omega} g_{\mu\chi} + g_{\mu\omega} g_{\nu\chi})] \\
& \times \epsilon_\phi^{*\zeta}(p_2) [g_{\mathcal{D}^* \mathcal{D}^* \psi} g_{\eta\gamma} g_{\psi\eta}^\eta(k_{1\zeta} + q_\zeta) \\
& - 4f_{\mathcal{D}^* \mathcal{D}^* \phi} p_2^\eta (g_{\gamma\eta} g_{\psi\zeta} - g_{\gamma\zeta} g_{\psi\eta})] \\
& \times \epsilon_\phi^{*\lambda}(p_3) [g_{\mathcal{D}^* \mathcal{D}^* \phi} g_{\rho\lambda} g_{\nu}^\rho (q_\lambda - k_{2\lambda}) \\
& - 4f_{\mathcal{D}^* \mathcal{D}^* \phi} p_3^\rho (g_{\rho\nu} g_{\nu\lambda} - g_{\rho\lambda} g_{\nu\rho})]. \quad (\text{E8})
\end{aligned}$$

[1] S. K. Choi *et al.* (Belle Collaboration), Observation of a Narrow Charmonium—Like State in Exclusive $B^\pm \rightarrow K^\pm \pi^+ \pi^- J/\psi$ Decays, *Phys. Rev. Lett.* **91**, 262001 (2003).

[2] N. Brambilla, S. Eidelman, P. Foka, S. Gardner, A. S. Kronfeld, M. G. Alford, R. Alkofer, M. Butenschoen, T. D. Cohen, and J. Erdmenger *et al.*, QCD and strongly

- coupled gauge theories: Challenges and perspectives, *Eur. Phys. J. C* **74**, 2981 (2014).
- [3] B. Aubert *et al.* (BABAR Collaboration), Observation of a Broad Structure in the $\pi^+\pi^-J/\psi$ Mass Spectrum Around 4.26-GeV/ c^2 , *Phys. Rev. Lett.* **95**, 142001 (2005).
- [4] B. Aubert *et al.* (BABAR Collaboration), Evidence of a Broad Structure at an Invariant Mass of 4.32-GeV/ c^2 in the Reaction $e^+e^- \rightarrow \pi^+\pi^-J/\psi$ Measured at BABAR, *Phys. Rev. Lett.* **98**, 212001 (2007).
- [5] X. L. Wang *et al.* (Belle Collaboration), Observation of Two Resonant Structures in $e^+e^- \rightarrow \pi^+\pi^-J/\psi(2S)$ via Initial State Radiation at Belle, *Phys. Rev. Lett.* **99**, 142002 (2007).
- [6] M. Ablikim *et al.* (BESIII Collaboration), Observation of a Charged Charmoniumlike Structure in $e^+e^- \rightarrow \pi^+\pi^-J/\psi$ at $\sqrt{s} = 4.26$ GeV, *Phys. Rev. Lett.* **110**, 252001 (2013).
- [7] M. Ablikim *et al.* (BESIII Collaboration), Observation of a Charged ($D\bar{D}^*$) $^\pm$ Mass Peak in $e^+e^- \rightarrow \pi D\bar{D}^*$ at $\sqrt{s} = 4.26$ GeV, *Phys. Rev. Lett.* **112**, 022001 (2014).
- [8] M. Ablikim *et al.* (BESIII Collaboration), Observation of a Charged Charmoniumlike Structure $Z_c(4020)$ and Search for the $Z_c(3900)$ in $e^+e^- \rightarrow \pi^+\pi^-h_c$, *Phys. Rev. Lett.* **111**, 242001 (2013).
- [9] M. Ablikim *et al.* (BESIII Collaboration), Observation of a Charged Charmoniumlike Structure in $e^+e^- \rightarrow (D^*\bar{D}^*)^\pm\pi^\mp$ at $\sqrt{s} = 4.26$ GeV, *Phys. Rev. Lett.* **112**, 132001 (2014).
- [10] S. K. Choi *et al.* (Belle Collaboration), Observation of a Resonance-Like Structure in the $\pi i^\pm\psi'$ Mass Distribution in Exclusive $B \rightarrow K\pi^\pm\psi'$ Decays, *Phys. Rev. Lett.* **100**, 142001 (2008).
- [11] M. Ablikim *et al.* (BESIII Collaboration), Future physics programme of BESIII, *Chin. Phys. C* **44**, 040001 (2020).
- [12] M. Ablikim *et al.* (BESII Collaboration), Observation of χ_{c1} Decays into Vector Meson Pairs $\phi\phi$, $\omega\omega$, and $\omega\phi$, *Phys. Rev. Lett.* **107**, 092001 (2011).
- [13] P. A. Zyla *et al.* (Particle Data Group), Review of particle physics, *Prog. Theor. Exp. Phys.* **2020**, 083C01 (2020).
- [14] C. N. Yang, Selection rules for the dematerialization of a particle into two photons, *Phys. Rev.* **77**, 242 (1950).
- [15] M. Ablikim *et al.* (BESIII Collaboration), Observation of OZI-suppressed decays $\chi_{cJ} \rightarrow \omega\phi$, *Phys. Rev. D* **99**, 012015 (2019).
- [16] V. L. Chernyak and A. R. Zhitnitsky, Exclusive decays of heavy mesons, *Nucl. Phys.* **B201**, 492 (1982); [Erratum, *Nucl. Phys.* **214**, 547 (1983)].
- [17] H. Q. Zhou, R. G. Ping, and B. S. Zou, Mechanisms for $\chi_{cJ} \rightarrow \phi\phi$ decays, *Phys. Lett. B* **611**, 123 (2005).
- [18] X. Liu, X. Q. Zeng, and X. Q. Li, Study on contributions of hadronic loops to decays of J/ψ to vector + pseudoscalar mesons, *Phys. Rev. D* **74**, 074003 (2006).
- [19] U. G. Meißner, Loop effects in charmonium transitions, *AIP Conf. Proc.* **1322**, 266 (2010).
- [20] F. K. Guo, C. Hanhart, G. Li, U. G. Meißner, and Q. Zhao, Effect of charmed meson loops on charmonium transitions, *Phys. Rev. D* **83**, 034013 (2011).
- [21] X. H. Liu and Q. Zhao, The evasion of helicity selection rule in $\chi_{c1} \rightarrow VV$ and $\chi_{c2} \rightarrow VP$ via intermediate charmed meson loops, *Phys. Rev. D* **81**, 014017 (2010).
- [22] D. Y. Chen, J. He, X. Q. Li, and X. Liu, Understanding the branching ratios of $\chi_{c1} \rightarrow \phi\phi$, $\omega\omega$, $\omega\phi$ observed at BES-III, *Phys. Rev. D* **81**, 074006 (2010).
- [23] F. K. Guo, C. Hanhart, G. Li, U. G. Meißner, and Q. Zhao, Novel analysis of the decays $\psi' \rightarrow h_c\pi^0$ and $\eta'_c \rightarrow \chi_{c0}\pi^0$, *Phys. Rev. D* **82**, 034025 (2010).
- [24] X. H. Liu and Q. Zhao, Further study of the helicity selection rule evading mechanism in η_c, χ_{c0} and h_c decaying to baryon antibaryon pairs, *J. Phys. G* **38**, 035007 (2011).
- [25] P. Colangelo, F. De Fazio, and T. N. Pham, $B \rightarrow K^-\chi_{c0}$ decay from charmed meson rescattering, *Phys. Lett. B* **542**, 71 (2002).
- [26] D. Y. Chen, X. Liu, and S. L. Zhu, Charged bottomoniumlike states $Z_b(10610)$ and $Z_b(10650)$ and the $\Upsilon(5S) \rightarrow \Upsilon(2S)\pi^+\pi^-$ decay, *Phys. Rev. D* **84**, 074016 (2011).
- [27] C. Meng and K. T. Chao, Scalar resonance contributions to the dipion transition rates of $\Upsilon(4S, 5S)$ in the re-scattering model, *Phys. Rev. D* **77**, 074003 (2008).
- [28] C. Meng and K. T. Chao, Peak shifts due to $B^*\bar{B}^*$ rescattering in $\Upsilon(5S)$ dipion transitions, *Phys. Rev. D* **78**, 034022 (2008).
- [29] D. Y. Chen, J. He, X. Q. Li, and X. Liu, Dipion invariant mass distribution of the anomalous $\Upsilon(1S)\pi^+\pi^-$ and $\Upsilon(2S)\pi^+\pi^-$ production near the peak of $\Upsilon(10860)$, *Phys. Rev. D* **84**, 074006 (2011).
- [30] D. Y. Chen, X. Liu, and T. Matsuki, Explaining the anomalous $\Upsilon(5S) \rightarrow \chi_{bJ}\omega$ decays through the hadronic loop effect, *Phys. Rev. D* **90**, 034019 (2014).
- [31] D. Y. Chen and X. Liu, $Z_b(10610)$ and $Z_b(10650)$ structures produced by the initial single pion emission in the $\Upsilon(5S)$ decays, *Phys. Rev. D* **84**, 094003 (2011).
- [32] C. Meng and K. T. Chao, $\Upsilon(4S, 5S)$ to $\Upsilon(1S)$ eta transitions in the rescattering model and the new BABAR measurement, *Phys. Rev. D* **78**, 074001 (2008).
- [33] X. Liu, B. Zhang, and X. Q. Li, The Puzzle of excessive non- $D\bar{D}$ component of the inclusive $\psi(3770)$ decay and the long-distant contribution, *Phys. Lett. B* **675**, 441 (2009).
- [34] G. Li, X. H. Liu, Q. Wang, and Q. Zhao, Further understanding of the non- $D\bar{D}$ decays of $\psi(3770)$, *Phys. Rev. D* **88**, 014010 (2013).
- [35] H. Y. Cheng, C. K. Chua, and A. Soni, Final state interactions in hadronic B decays, *Phys. Rev. D* **71**, 014030 (2005).
- [36] Y. A. Simonov and A. I. Veselov, Bottomonium dipion transitions, *Phys. Rev. D* **79**, 034024 (2009).
- [37] D. Y. Chen, Y. B. Dong, and X. Liu, Long-distant contribution and χ_{c1} radiative decays to light vector meson, *Eur. Phys. J. C* **70**, 177 (2010).
- [38] G. Li, Q. Zhao, and B. S. Zou, Isospin violation in $\phi, J/\psi, \psi' \rightarrow \omega\pi^0$ via hadronic loops, *Phys. Rev. D* **77**, 014010 (2008).
- [39] G. Li and Q. Zhao, Revisit the radiative decays of J/ψ and $\psi' \rightarrow \gamma\eta_c(\gamma\eta'_c)$, *Phys. Rev. D* **84**, 074005 (2011).
- [40] H. Chen and R.-G. Ping, Polarization in $\chi_{cJ} \rightarrow \Lambda\bar{\Lambda}$ decays, *Phys. Rev. D* **102**, 016021 (2020).
- [41] M. G. Doncel, P. Mery, L. Michel, P. Minnaert, and K. C. Wali, Properties of polarization density matrix in Regge-pole models, *Phys. Rev.* **7**, 815 (1973).

- [42] R. Casalbuoni, A. Deandrea, N. Di Bartolomeo, R. Gatto, F. Feruglio, and G. Nardulli, Phenomenology of heavy meson chiral Lagrangians, *Phys. Rep.* **281**, 145 (1997).
- [43] O. Kaymakcalan, S. Rajeev, and J. Schechter, Nonabelian anomaly and vector meson decays, *Phys. Rev. D* **30**, 594 (1984).
- [44] Y. s. Oh, T. Song, and S. H. Lee, J/ψ absorption by π and ρ mesons in meson exchange model with anomalous parity interactions, *Phys. Rev. C* **63**, 034901 (2001).
- [45] H. Y. Cheng, C. Y. Cheung, G. L. Lin, Y. C. Lin, T. M. Yan, and H. L. Yu, Chiral Lagrangians for radiative decays of heavy hadrons, *Phys. Rev. D* **47**, 1030 (1993).
- [46] T. M. Yan, H. Y. Cheng, C. Y. Cheung, G. L. Lin, Y. C. Lin, and H. L. Yu, Heavy quark symmetry and chiral dynamics, *Phys. Rev. D* **46**, 1148 (1992).
- [47] M. B. Wise, Chiral perturbation theory for hadrons containing a heavy quark, *Phys. Rev. D* **45**, R2188 (1992).
- [48] G. Burdman and J. F. Donoghue, Union of chiral and heavy quark symmetries, *Phys. Lett. B* **280**, 287 (1992).
- [49] A. F. Falk and M. E. Luke, Strong decays of excited heavy mesons in chiral perturbation theory, *Phys. Lett. B* **292**, 119 (1992).
- [50] C. Itzykson and J. B. Zuber, *Quantum Field Theory*, International Series In Pure and Applied Physics (Mcgraw-hill, New York, USA, 1980), p. 705.
- [51] M. E. Peskin and D. V. Schroeder, An introduction to quantum field theory.
- [52] O. Gortchakov, M. P. Locher, V. E. Markushin, and S. von Rotz, Two meson doorway calculation for $\bar{p}p \rightarrow \phi\pi$ including off-shell effects and the OZI rule, *Z. Phys. A* **353**, 447 (1996).
- [53] A. V. Manohar and M. B. Wise, Heavy quark physics, Cambridge Monogr. Part. Phys., Nucl. Phys., Cosmol. **10**, 1 (2000).
- [54] M. Neubert, Heavy quark symmetry, *Phys. Rep.* **245**, 259 (1994).
- [55] C. Isola, M. Ladisa, G. Nardulli, and P. Santorelli, Charming penguins in $B \rightarrow K^*\pi, K(\rho, \omega, \phi)$ decays, *Phys. Rev. D* **68**, 114001 (2003).
- [56] L. Burakovsky and J. T. Goldman, Gell-Mann-Okubo mass formula revisited, [arXiv:hep-ph/9708498](https://arxiv.org/abs/hep-ph/9708498).
- [57] A. Kucukarslan and U. G. Meißner, Omega-phi mixing in chiral perturbation theory, *Mod. Phys. Lett. A* **21**, 1423 (2006).
- [58] M. Benayoun, L. DelBuono, S. Eidelman, V. N. Ivanchenko, and H. B. O'Connell, Radiative decays, nonet symmetry and SU(3) breaking, *Phys. Rev. D* **59**, 114027 (1999).
- [59] S. I. Dolinsky, V. P. Druzhinin, M. S. Dubrovin, V. B. Golubev, V. N. Ivanchenko, E. V. Pakhtusova, A. N. Peryshkin, S. I. Serednyakov, Y. M. Shatunov, and V. A. Sidorov *et al.*, Summary of experiments with the neutral detector at the $e + e -$ storage ring VEPP-2M, *Phys. Rep.* **202**, 99 (1991).
- [60] L. B. Chen and C. F. Qiao, P-wave quarkonium decays to meson pair, *J. High Energy Phys.* **11** (2012) 168.
- [61] H. Chen and R. G. Ping, Polarization in $\chi_{cJ} \rightarrow \phi\phi$ decays, *Phys. Rev. D* **88**, 034025 (2013).
- [62] M. Ablikim *et al.* (BESIII Collaboration), Observation of the helicity-selection-rule suppressed decay of the χ_{c2} charmonium state, *Phys. Rev. D* **96**, 111102 (2017).